8-2010

A General Simulation of an Air Ejector Diffuser System

Derick Thomas Daniel
University of Tennessee - Knoxville, derick.daniel@arnold.af.mil

To the Graduate Council:

I am submitting herewith a thesis written by Derick Thomas Daniel entitled "A General Simulation of an Air Ejector Diffuser System." I have examined the final electronic copy of this thesis for form and content and recommend that it be accepted in partial fulfillment of the requirements for the degree of Master of Science, with a major in Mechanical Engineering.

Gary A. Flandro, Major Professor

We have read this thesis and recommend its acceptance:

Trevor Moeller, John S. Steinhoff

Accepted for the Council:
Carolyn R. Hodges

Vice Provost and Dean of the Graduate School

(Original signatures are on file with official student records.)

To the Graduate Council:

I am submitting herewith a thesis written by Derick Thomas Daniel entitled "A General Simulation of An Air Ejector Diffuser System." I have examined the final electronic copy of this thesis for form and content and recommend that it be accepted in partial fulfillment of the requirements for the degree of Master of Science, with a major in Mechanical Engineering.

Gary Flandro , Major Professor

We have read this thesis
and recommend its acceptance:

Trevor Moeller

John Steinhoff

Accepted for the Council:

Carolyn R. Hodges
Vice Provost and Dean of the Graduate School

(Original signatures are on file with official student records.)

A General Simulation of An Air Ejector Diffuser System

A Thesis
Presented for the
Master of Science
Degree
The University of Tennessee, Knoxville

Derick Thomas Daniel
August 2010

DEDICATION

This thesis is dedicated to my family—Mitchell, Vickey, Chastie, and Gabriela. Each one of them has been a major part of my success and happiness in both my life and my career.

ACKNOWLEDGEMENTS

My gratitude is extended to all of the wonderful people that helped guide me during this thesis. Dr. Rob McAmis was instrumental in the progression of my studies at UTSI as well as the progression of this thesis. He helped guide me to the thesis topic presented here, and I am grateful for his help and his careful guidance throughout my time at UTSI. The thesis topic chosen was suggested by Brent Bates, and his technical knowledge of facility modeling was an immense resource for me. Andy Escue also was a great help for his knowledge of the facility computer models in Matlab/Simulink. I had previously worked with both Brent Bates and Andy Escue on improvements to the facility computer models, and they have always been extremely helpful and inspiring to work with. I also would like to thank the members of my thesis committee. Dr. Gary Flandro provided much useful insight and help in the development of this thesis. Not only was his help during this thesis important, but his compressible flow classes that I attended previously were a huge resource that I pulled from extensively. Dr. John Steinhoff and Dr. Trevor Moeller were also a great help to me, and I would like to thank all of my thesis committee members and others who helped me with their knowledge and support. Besides these people already mentioned, I would like to thank Arnold Air Force Base and all the people there that helped me directly or indirectly in some way.

ABSTRACT

A computer model of a blow-down free-jet hypersonic propulsion test facility exists to validate facility control systems as well as predict problems with facility operation. One weakness in this computer model is the modeling of an air ejector diffuser system. Two examples of facilities that could use this ejector diffuser model are NASA Langley Research Center's 8-ft High Temp. Tunnel (HTT) and the Aero-Propulsion Test Unit (APTU) located at Arnold Engineering Development Center. Modeling an air ejector diffuser system for a hypersonic propulsion test facility includes modeling three coupled systems. These are the ejector system, the primary free-jet nozzle that entrains secondary airflow from the test cell, and the test article. Both of these facilities are capable of testing scramjets/ramjets at high Mach numbers. Compared with computer simulation data, experimental test cell pressure data do not agree due to the current modeling technique used.

An improved computer model was derived that incorporates new techniques for modeling the ejector diffuser. This includes real gas effects at the ejector nozzles, flow constriction due to free-jet nozzle and ejector plumes, test article effects, and a correction factor of the normal shock pressure ratio in a supersonic diffuser. A method was developed to account for the drag and thrust terms of the test article by assuming a blockage factor and using a drag coefficient*Area term for both the test article and thrust stand derived from experimental data. An ideal ramjet model was also incorporated to account for the gross thrust of the test article on the system.

The new ejector diffuser model developed improved the accuracy and fidelity of the facility model as compared with experimental test data while only negligibly affecting computational speed. Comparisons of the model data with experimental test data showed a close match for test cell pressure (within 1 percent for final test cell pressure). The model accurately simulated both the unstarted and started modes of ejector flow, in which test cell pressure increases with nozzle total pressure once in started mode.

TABLE OF CONTENTS

LIST OF FIGURES

LIST OF SYMBOLS

Symbol	Definition
a	speed of sound
A	area (in^2)
AR	nozzle exit to throat area ratio
c_d	drag coefficient
c_f	flow coefficient
c_p	constant pressure specific heat capacity
c_v	constant volume specific heat capacity
D	drag force
Δ	delta
η_P	ram/scramjet propulsive efficiency
η_T	ram/scramjet thermal efficiency
F	force
f	fuel air ratio
F_{GROSS}	test article gross thrust
F_{NET}	test article net thrust
γ	ratio of specific heats (c_p/c_v)
g_c	gravitational constant
m	mass
M	Mach number
$\dot{m}$	mass flow
P	static pressure

P_t	total pressure
Q	dynamic pressure
R	gas constant
ρ	density
S	thrust specific fuel consumption
T	static temperature
τ	total to static temperature ratio
T_t	total temperature
V	volume
v	velocity

1. INTRODUCTION

The general facility discussed in this paper is a blow-down free-jet hypersonic propulsion test facility that is made up of many components. High pressure air from high pressure storage bottles will be modeled as the supply source for the ejector flow and the free-jet nozzle flow. The storage of the supply air limits continuous operation to short durations only. The supply air is heated prior to entering a free-jet nozzle which provides the high temperature and Mach number airflow to the test article. It is assumed that the air is heated without affecting the mole fractions of its constituents. The free-jet nozzle is a fixed area nozzle that is designed for a specific Mach number flow, and for this analysis, a nozzle designed for a Mach number of 4.5 will be modeled.

The main purpose of a diffuser is to slow the airflow with as small a loss of total pressure as possible while increasing the static pressure before exhausting to atmosphere. Subsonic diffusers such as in wind tunnels slow the airflow and increase static pressure by a change in the duct area in which the airflow passes. However, supersonic exhaust diffusers for propulsion testing are more complex. They capture high energy supersonic exit flow and accomplish diffusion through a process of turbulent mixing and multiple shock systems involving a combination of normal and/or oblique shocks. Supersonic exhaust diffusers are typically used in altitude simulation of rocket, turbine, and ramjet/scramjet engines. Unlike subsonic diffusers, supersonic diffusers such as the cylindrical diffuser do not require an area change because the system of shocks accomplishes the increase in static pressure. Three common types of supersonic diffusers

used are the cylindrical, short second throat, and long second throat diffuser [13]. The diffuser to be modeled in this paper is a cylindrical diffuser, or constant area diffuser.

Ejectors are simple pumps which are often used in favor of reciprocating or rotary compressors where hot gases are handled such as combustion gases exhausted by rocket or turbine engines. Ejectors work using the momentum exchange in the boundary layer created by a primary high velocity air stream and a secondary lower velocity air stream. A simple schematic of an ejector system is shown in Figure 1. Essentially, a rocket or turbine engine acts as an ejector in a typical free jet test cell, using its high velocity exhaust gases to entrain airflow around the engine to lower the static pressure in the test cell. Figure 2 is a depiction of the general system being modeled. It consists of a free-jet nozzle and shroud which act as an ejector diffuser system alone. Just downstream of the nozzle is the test article whose exhaust gases would also entrain air similar to an ejector. Further downstream past the shroud, a system of axi-symmetric annular ejectors is used as the main ejector system. This ejector system is used to attain low test cell pressure prior to the free-jet nozzle operation to help start the free-jet nozzle and to attain lower pressures than possible with the free-jet nozzle only.

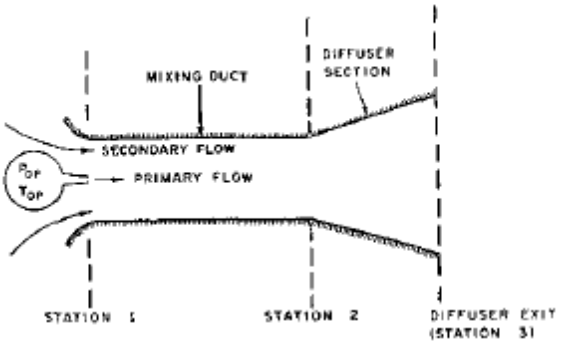

Figure 1: Simple Ejector Diffuser Schematic [1]

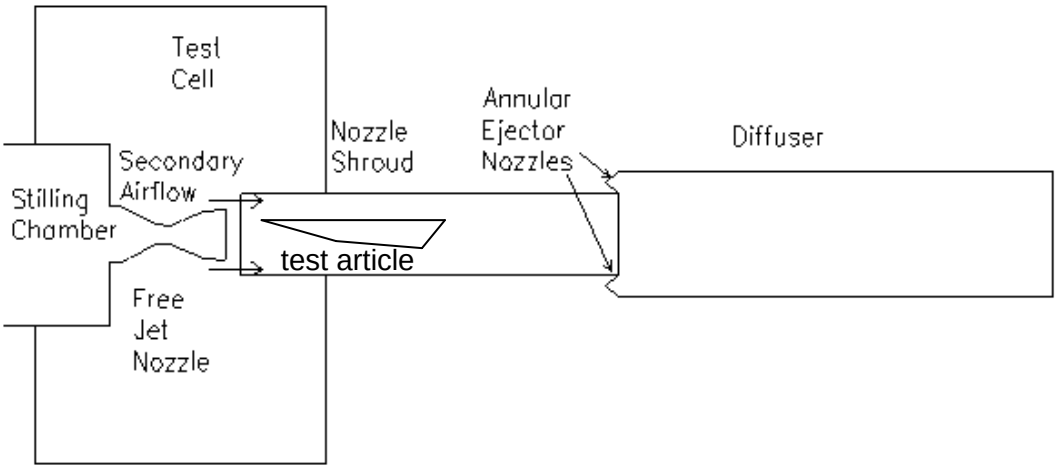

Figure 2: Ejector Diffuser System Modeled

Ejectors have two main modes of operation; started and un-started. On Figure 3, section 1 represents the un-started mode and section 3 represents the started mode. During the un-started mode, the nozzle flow has not attached to the wall of the diffuser, thus the secondary flow and nozzle flow are separate, and increasing nozzle pressure results in an increase in entrainment rate of the secondary flow. As operation moves along section 2, there is a very large decrease in P/Pt ratio for a small change in Pex/Pt which leads to the started mode of operation. When operation is in this mode, the driving pressure is adequate to fully expand the supersonic nozzle flow, and the attachment point on the diffuser wall is close to the nozzle and is fairly stable. At this point, there is a minimum Pc/Pt ratio which remains constant, and Pc (test cell pressure) will be a function of Pt (nozzle total pressure) only. Further increase of nozzle pressure after entering a started mode will increase test cell pressure instead of decreasing it.

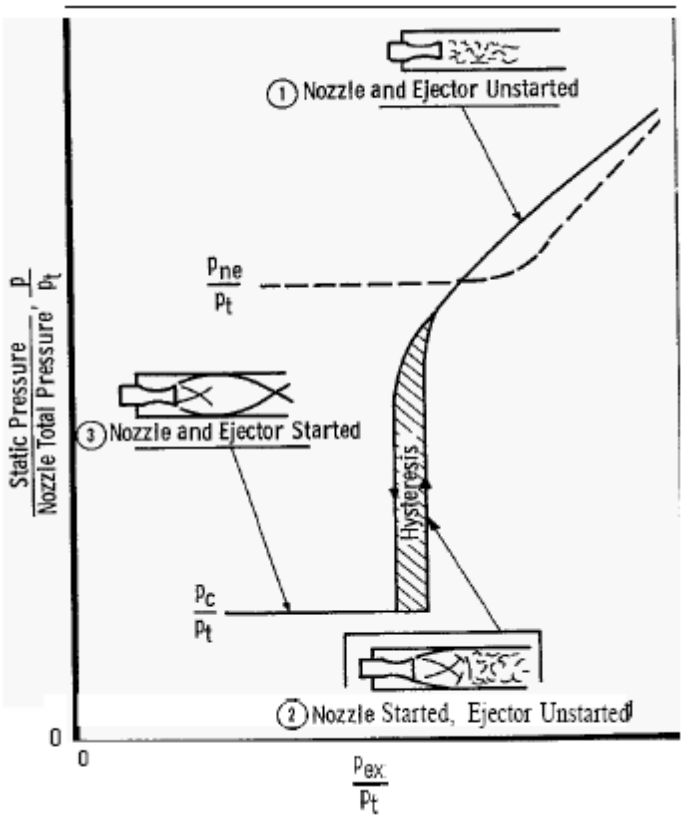

Pt – nozzle total pressure

Pex – diffuser exit static pressure

P – test cell static pressure

Figure 3: Ejector Performance [8]

2. PROBLEM STATEMENT

A detailed computer model in Mathwork's Matlab/Simulink® environment was developed that mathematically represents the process physics of a blow-down hypersonic propulsion test facility's subsystems. In order for the model to be useful in validating a facility's control system, the model needs to be fast enough to run as a real time simulation. The model can then be used as a desktop version and also a compiled real time version. The real time version would then be able to receive control by communicating with the actual control system PLC's while the desktop version would use a PID controller model to input these commands. The current simulation data compared with experimental data has shown that test cell pressure does not closely match. The subsystem simulation that does not accurately predict the problem physics is the ejector diffuser system. The ejector diffuser modeled is a coupled system of the primary free-jet nozzle assembly and shroud, test article, and annular ejector system and diffuser. The main challenge and goal is calculating the secondary flow from the test cell. All other flow quantities (nozzle flow, annular ejector flow) are calculated and known because they generally operate choked and thus are independent of the downstream pressures which are unknown. An estimated constant area is assumed for the leakage into the test cell and the leakage flow is calculated from a simple orifice calculation. Thus, being able to calculate the secondary airflow, the test cell pressure can then be calculated as well. Predicting this test cell pressure more accurately is the main objective of modeling the ejector diffuser system.

3. LITERATURE SEARCH

Several methods of calculating ejector diffuser performance have been used. The main methods are one dimensional analysis [4], the method of characteristics [13], and finite difference methods [12]. Most of the literature reviewed used a one dimensional approach to modeling an ejector diffuser. The latter approaches require significant computer time to calculate and are more sensitive to the geometry of the ejector diffuser system and test article. Thus, the one dimensional analysis seems to be well-suited for computer simulation and the integration into a larger one dimensional facility model.

Bauer, Muse, and Tinsley [2] used this 1-D approach to simulate a hypersonic test facility. Several commonly used assumptions were made that included steady flow, ideal gas, no test vehicle engine operation, diffuser length sufficient for complete mixing, 1-D secondary flow from test cell, test cell pressure being the total pressure of the secondary flow, and no flow separation in the facility nozzle. A momentum balance of a control volume was used in which the sum of the forces on the system is zero. They noted that limitations to using this analysis were imposed by boundary layer separation, diffuser choking, jet pluming, and base flow phenomena. Therefore, minimum test cell pressure is limited by the latter three conditions. Diffuser choking can be easily predicted using the 1-D approach and is defined by the choking of the secondary flow around the nozzle. However, the test article introduces a blockage factor that will increase the test cell pressure at which the diffuser chokes.

Another complication is jet pluming, which occurs when the diffuser inlet is located at a significant distance downstream of the nozzle exit. As test cell pressure is decreased, the nozzle plume diameter increases to fill the diameter of the diffuser. Therefore, based on a conservation of mass, the lowest test cell pressure is the one in which the nozzle plume has filled the entire inlet diameter of the diffuser. When the distance between the nozzle exit and diffuser inlet is decreased, then another effect known as base flow phenomena becomes important. This occurs when the plume attaches itself to the internal surface of the diffuser and only occurs when the diffuser inlet is sufficiently far upstream of the plume attachment point. It is also worth noting that the minimum chamber pressure produced by the base flow limit is significantly less than that produced by the pluming limit. Bauer [2] also mentions that for optimum performance, the test article should not block the flow to exceed the normal shock limits (constrict supersonic flow down to sonic conditions).

German and Bauer [3] investigated the effect of diffuser length with different configurations on ejector performance. It was stated that investigations of constant area cylindrical supersonic diffusers have shown that the pressure rise (test cell-to-diffuser exit) follows closely the normal shock static pressure rise. Empirical data was compiled for cylindrical diffusers as a function of geometry, and this data is shown in figure 4. It is shown from this data that true pressure recovery in a cylindrical diffuser with a "bell" nozzle and $L/D \geq 8$ is 80% of the normal shock pressure recovery. The following plot shows this empirical data for different geometries. This recovery factor includes the effects of the viscous boundary layer as well as the complex system of oblique shocks in the diffuser. In our ejector diffuser system, the primary free-jet nozzle is a bell nozzle,

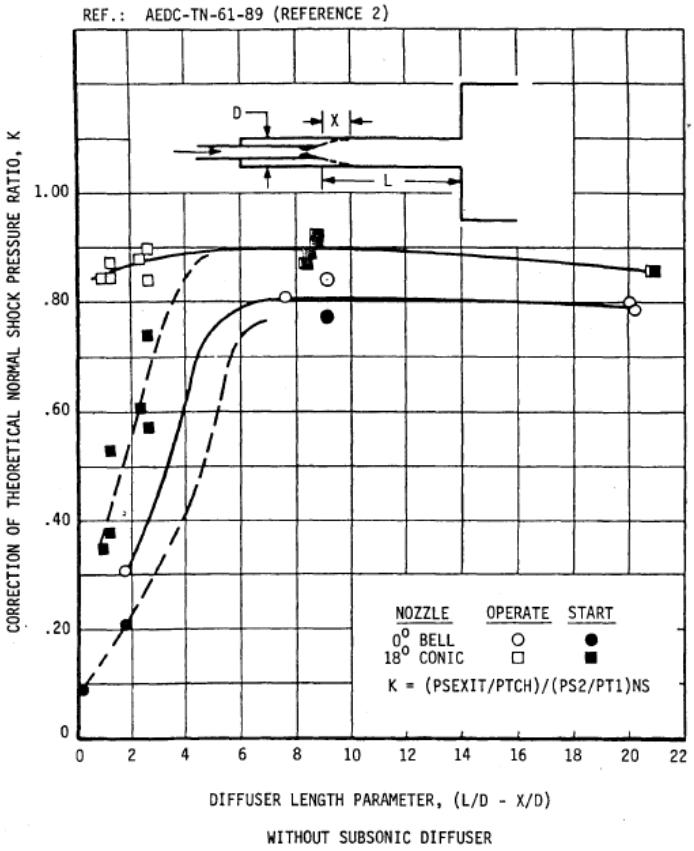

Figure 4: Correction of Theoretical Normal Shock Pressure Ratio [3]

and the ejector is a conical nozzle which has a correction factor of approx. 90% based on Figure 4. The conical nozzles have a higher pressure recovery since they have nearly isentropic expansion as compared to a bell nozzle.

Dutton [4] conducted a one dimensional analysis and presented a solution method for finding the secondary flow, as well as the minimum secondary to primary flow pressure ratio. This analysis is based on the choking of the secondary flow due to its compression by the free-jet plume. In this analysis, it is assumed that the free-jet nozzle expands isentropically in an inviscid interaction region. In this region, each stream remains separate and may have a different static pressure. The free-jet nozzle flow

expands out until the static pressures are equal which is where the mixing region begins. This creates an aerodynamic throat (choke point) of the secondary flow. In reality, the streams must maintain the same static pressure at the slip line between the two streams. Dutton [4] also performed experiments to test the theory. He concluded that an empirical correction factor of about 0.8 would bring the theoretical data to within a few percent of experimental data. His experiments were based on only large L/D ratios that were sufficient for mixing. This agrees well with values attained by German [3] in the previous plot (Figure 4). Also, Dutton's experiments showed that at high primary to secondary pressure ratios, that flow separation occurred for the secondary flow. This limits ejector performance and increases the error associated with one dimensional analysis. Similar conclusions have been made in other papers [2] about degradation of performance due to flow separation.

Luce [5] formulated a calculation method to approximate plume sizes for nozzle flow. This may prove to be a useful tool as well in determining diffuser choking due to the nozzle plume. However, the current simulation data indicates an over-expanded nozzle which actually creates a contraction instead of an expansion of the nozzle exit flow. This will not always be the case for different configurations such as free-jet nozzles designed for different Mach numbers.

The two-dimensional supersonic base pressure theory was developed by Dr. Korst and was modified by Bauer [6] to be more accurate for axi-symmetric ejector systems. The theory provides a method to determine total pressure at the dividing streamline in the mixing zone between nozzle and secondary flow. The method is described in German and Bauer's paper and is computationally more intensive due to using the method of

characteristics. Ferri [7] describes in more detail the process of calculating the nozzle plume shape either by the method of characteristics or simply with prandtl-meyer expansion and compression shocks.

3.1 CONCLUSIONS OF THE LITERATURE SEARCH

Several methods for approximating ejector diffuser performance exist that could have been appropriate for the computer model addressed in this thesis. The least computationally intensive methods are the one dimensional analysis and are the most practical for integrating into a larger dynamic computer model. However, they also provide less detail of the flow than a finite difference method. Minimum test cell pressure ratio is determined by diffuser choking at the secondary flow entrance, diffuser exit, or internally (Primary Stream Pressure > Secondary Stream Pressure). Internal diffuser choking is caused by the pluming of the flow from the nozzle exit, thus causing a constriction in the secondary flow that causes it to choke. A conservative estimate of the onset of internal diffuser choking occurs when nozzle exit pressure is equal to the secondary flow pressure (test cell pressure) for diffusers not much larger than the nozzle exit [8]. A more accurate estimate of diffuser choking can be calculated using the method of characteristics, which is computationally intensive and shows much of the details of the flow. The minimum test cell pressure ratio due to diffuser choking can then be used in a one dimensional simulation to determine when the nozzle/ejector flow is in the started condition. Once in a started condition, primary to secondary flow static pressure ratio is constant and no longer requires a momentum balance to calculate. Most of the papers researched used a momentum balance of all the flows into and out of the

diffuser and assumed completely expanded flow to ambient pressure at the diffuser exit. These calculations also typically assumed a normal shock recovery and used a correction factor based on empirical data of 0.8-0.9 for most cylindrical diffusers.

4. BACKGROUND – PREVIOUS EJECTOR DIFFUSER MODEL

The detailed computer model constructed in Mathwork's Matlab/Simulink® environment, that was developed to mathematically represent the process physics of an entire test facility is wrapped around an S-Function used to simulate the ejector diffuser subsystem. Simulink is a commercial tool used for modeling dynamic systems and is highly integrated with Matlab. It uses a block diagram system for creating dynamic simulations, and S-functions are simply user defined function blocks that can be written in a variety of languages (C, Fortran, Matlab) and compiled by Matlab. The ejector diffuser S-function's main purpose is to calculate mass flow leaving the test cell through the diffuser due to flow entrainment. A calculation of test cell leakage is performed outside this S-function which uses the delta pressure (atmospheric ambient – test cell) and an estimate of constant leakage area through an orifice. These calculations are done for every time step of the simulation which allows the total mass of the test cell to be calculated, and thus the static pressure can be determined. Knowing the accurate static pressure of the test cell is critical to calculating the test rhombus of the nozzle flow. The test rhombus is comprised of the oblique shocks which are reflected by the wall of the nozzle exit. The location and size of the test rhombus is important because the test article inlet must reside inside the test rhombus (see Appendix-A Figure 29) to avoid shock interactions with its inlet [2]. This is the primary reason to calculate an accurate test cell pressure, since the control system does not control to a test cell pressure in the current model.

Several weaknesses were discovered in the previous model and will be explained herein. The previous ejector-diffuser model is a 1-D mass & momentum balance with no real gas effects that calculates the static pressure rise of the diffuser across a normal shock. Also, the effects of the test article are ignored in the current model. This was partially justified by the fact that the drag term of the test article would act to offset some of the thrust from the engine. This is not a good assumption, especially when the test article isn't running. The model uses a force balance method in which the force acting on the air at the diffuser exit equals the sum of the airflow streams feeding into the system. These airflows are the ejector flow, free-jet nozzle flow, and secondary airflow from the test cell. Knowing the total force and mass flow at the diffuser exit, along with the ideal gas and momentum equation, static pressure at the exit can then be calculated. Two major components contribute to changing static pressure. Increasing the force of the airflows will increase the static pressure. However, increasing mass flow causes static pressure to decrease at a faster rate. This is important in how the program calculates secondary air flow.

Initially, the previous model assumes that the secondary airflow into the shroud is choked and calculates the mass flow and force of the flow. It uses the difference between the shroud and nozzle area as the secondary flow area. The force and mass flow of the free-jet nozzle is calculated using ideal gas assumption and input into this ejector diffuser model. Due to the high temperatures and reasonably low pressures of the free jet nozzle inlet, the ideal gas assumption is a good approximation. However, the ejector force and mass flow is calculated using an ideal gas nozzle approach, and there could be significant error in this calculation due to very high ejector manifold pressures and low temperatures.

These mass flows and forces are summed at the diffuser exit to find static pressure. If this static pressure is greater than or equal to ambient pressure, it is assumed that the secondary flow is indeed choked, and it stops the calculation.

The calculation is stopped because increasing secondary mass flow decreases diffuser exit static pressure, so further pressure decrease is impossible since the choked flow is the maximum flow attainable. In the original model, it is also assumed that the diffuser is subsonic at the exit and the flow completely expands to ambient pressure. So, if diffuser exit static pressure is calculated to be lower than ambient pressure, then reducing mass flow to a value less than the choked flow value will increase the diffuser exit static pressure closer to ambient pressure. The model then iterates between the maximum and minimum secondary airflow possible (forward choked flow & reverse choked flow respectively) until either diffuser exit pressure equals ambient pressure or until airflow has converged. This method of solution is used to calculate scenarios where free-jet nozzle is on and ejector flow is off or on. A slightly different method that uses the same principle is implemented when the ejectors are on and the free-jet nozzle is off.

During a typical test, the annular ejector system would be initiated prior to initiating the free-jet nozzle flow. When only the ejectors are in operation, highly irregular output is produced with the current model. A large downward spike in pressure occurs that is not obviously explained by the pressures and temperatures of the system. This will need to be addressed during the analysis performed in this thesis. After the free-jet nozzle flow has started, the code described in the previous paragraph is used. With this routine, the secondary airflow was found to become choked immediately upon the start of the free-jet nozzle. Since the choked flow only then depends upon the

upstream pressure or test cell pressure, the secondary airflow and test cell pressure become constant. Any changes in ejector flow or free-jet nozzle flow would not alter test cell pressure until total flows were reduced enough to stop the choking condition of the secondary flow. In reality, the started regime should follow the minimum constant test cell pressure/nozzle total pressure ratio. This would increase test cell pressure for further increases in nozzle total pressure.

Another assumption used in the existing model that has significant error is the assumption that the pressure recovery through the diffuser is that across a normal shock. This error results because a supersonic diffuser has a complex series of oblique shocks which give a pressure recovery less than that of a normal shock. Output from this program shows that the mass flow and force from the ejectors is much larger than airflow from the secondary flow. Using the force balance method, this makes secondary airflow extremely sensitive to the force and mass flow calculated from the ejectors. So errors in ejector mass flow and force due to incorrect throat area, ideal gas assumption, and two phase flows could be significant and cause the secondary mass flow calculated to be incorrect. The simulation is predicting a choking of secondary air flow where experimental data shows it is not. This suggests that the force at the diffuser exit is higher than it should be which is reasonable due to the absence of a diffuser normal shock pressure recovery correction term.

Figure 5 below shows non-dimensionalized data from the current computer model. As shown here, test cell pressure dives downward momentarily during ejector only flow. Also, the test cell secondary airflow immediately chokes after the free jet nozzle has been started. Once the secondary airflow chokes, the test cell pressure stays

constant and no longer responds to the increases in ejector or free-jet nozzle flow. In figure 6, experimental data is shown for the ejector diffuser system. This data shows that no downward spike in test cell pressure exists prior to the free jet nozzle starting. It also shows that the test cell secondary airflow does not immediately choke once the free jet nozzle has started. After the system enters a started mode as in Figure 3, the test cell pressure becomes a function of a constant pressure ratio (test cell static pressure / free-jet nozzle total pressure = constant) since the ejector pressures are relatively constant. This results in the test cell pressure increasing as the free-jet nozzle total pressure increases. This started condition phenomena does not occur in the previous ejector diffuser simulation (constant test cell pressure), but it will be shown in the new simulation data as well as the experimental data.

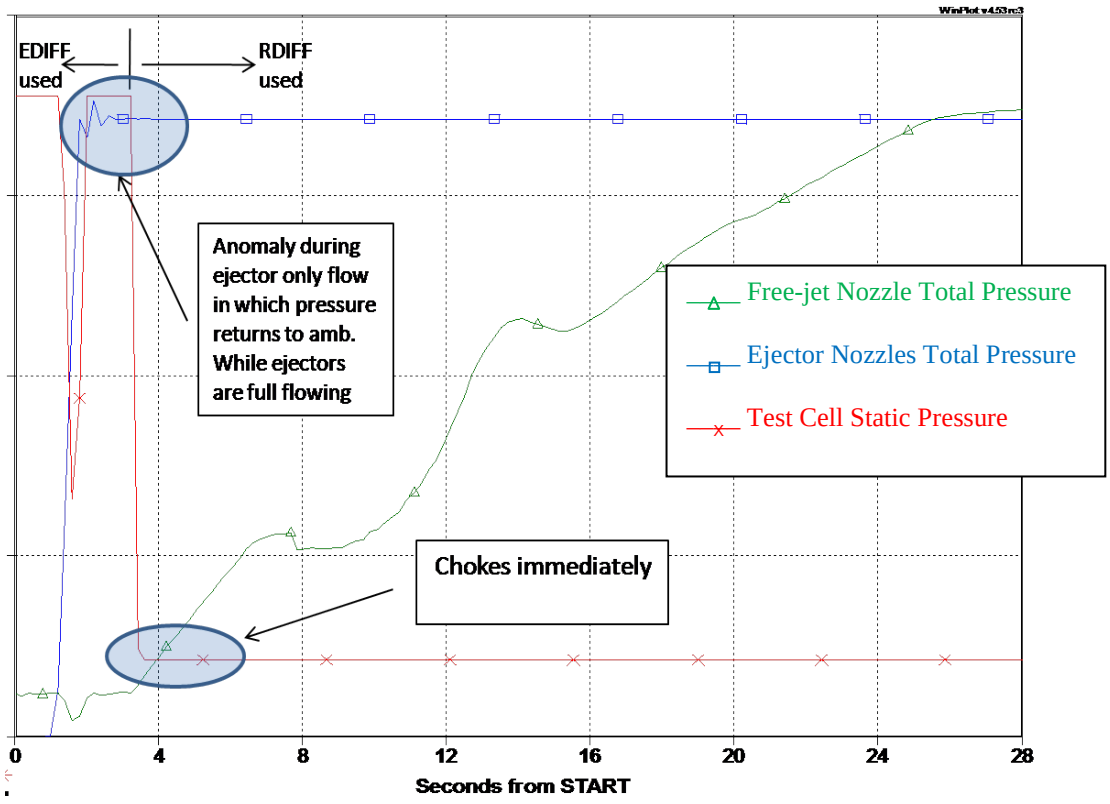

Figure 5: Previous Ejector Diffuser Simulation Output

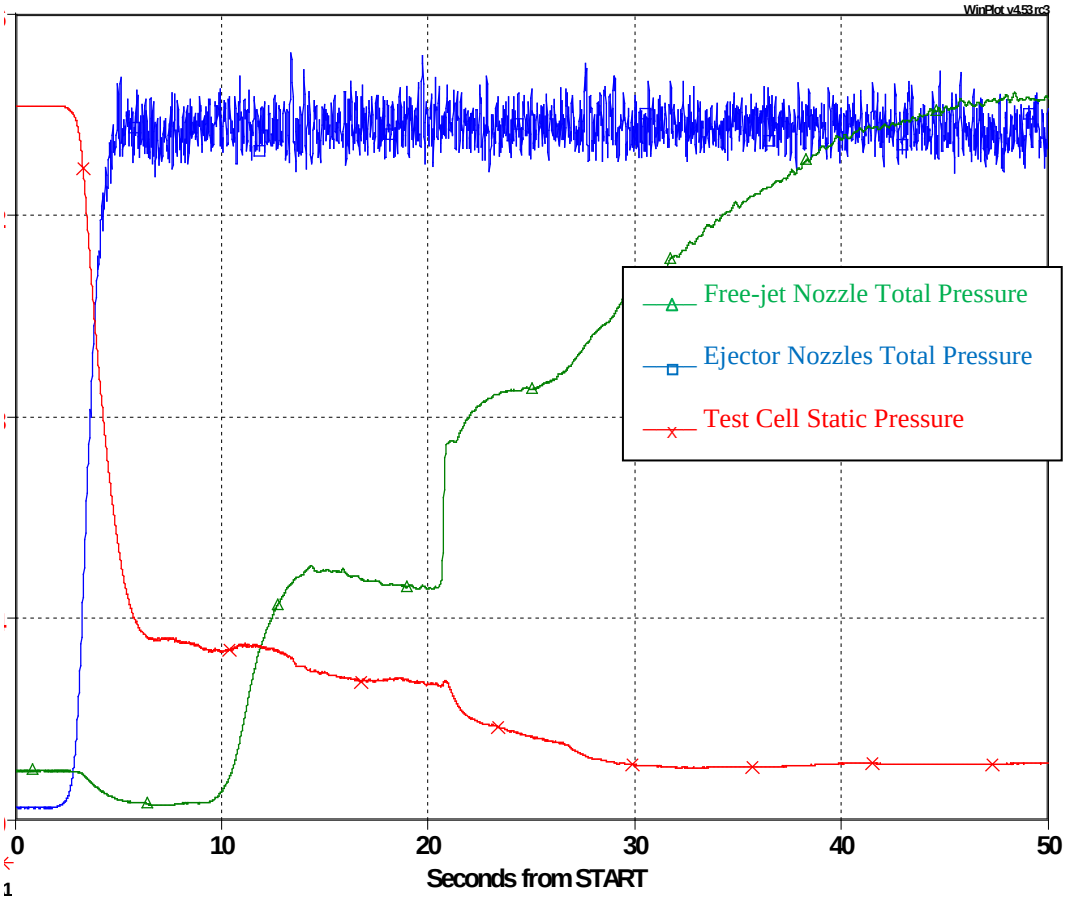

Figure 6: Experimental Facility Pressure Data

5. APPROACH

5.1 OUTLINE

The following is an outline of the approach used to develop an updated model of the ejector diffuser system:

1. Analyzed the current 1-D ejector diffuser model.
    a. Re-derived and verified equations used in current model and determined assumptions used.
    b. Determined if assumptions and current input data were really valid and approximated errors associated with these assumptions
        i. Ejector flows (high pressure, low temperature)
            1. Ideal gas vs. real gas for high pressure, low temp. ejector flows
            2. Two phase vs. one phase flow effects
            3. Throat area and exit area
            4. Un-started/Started operation
        ii. Diffuser and Shroud
            1. No drag vs. drag
            2. Ideal expansion to ambient pressure at exit
        iii. Secondary Flow from Test Cell
            1. 1-D flow

2. Assumed Test Cell Leakage Area
3. Max. flow is based on choking of (shroud area minus free-jet nozzle exit area) or internal choking (shroud area minus max. nozzle plume area)

c. Made different assumptions as necessary

d. Derived and used new equations associated with changed assumptions

2. Determined started and un-started operation boundaries for ejector flow and free-jet nozzle flow

3. Introduced a simplified way to account for diffuser blockage due to test article as well as an approximate force and drag term using prior test data.

5.2 CALCULATION SCHEME

5.2.1 OVERVIEW

In order to have a robust computer model that can both handle transient and steady state response of the ejector diffuser system, it is necessary to use various different subroutines which calculate all the possible flow regimes of the system. The updated computer model can be essentially broken down into three subsystems linked together. The first subsystem is the free jet nozzle feeding air to the test article, and the entrained secondary airflow from the test article. These two flows proceed down the nozzle shroud around and through the test article. The test article is the second system and adds a drag and thrust term, as well as changing the air properties of the mixed flow downstream.

The flows from the test cell, free jet nozzle, and test article then proceed into the diffuser where they are further entrained by the third system, the ejectors. Each of these systems affects the others through flow constriction and the energy they add to the total flow.

The free jet nozzle flow is calculated in the facility model outside of the main ejector diffuser model discussed in this paper. This free jet model uses upstream air properties and nozzle geometry data to calculate five different flow regimes: unchoked, choked with contained shock, choked supersonic, unchoked with backflow, and choked with backflow. The outputs from this model that are input into the ejector diffuser system model are the thrust of the nozzle and the static pressure and temperature at the exit plane.

The test cell is modeled as a control volume with an orifice flow simulating leakage from atmosphere into the test cell and the secondary flow going through the diffuser (see Figure 7). These flows are summed to get a total mass in the test cell and thus a static pressure can be calculated. Since the leakage flow can be easily determined, the only unknown is the secondary flow leaving the test cell through the diffuser. Therefore, this mass flow must be determined because the main purpose of modeling the ejector diffuser system is to calculate this static pressure. Inputs into the atmosphere leakage to test cell orifice flow are a nominal leakage area, a flow coefficient, test cell volume, atmospheric pressure, and air properties.

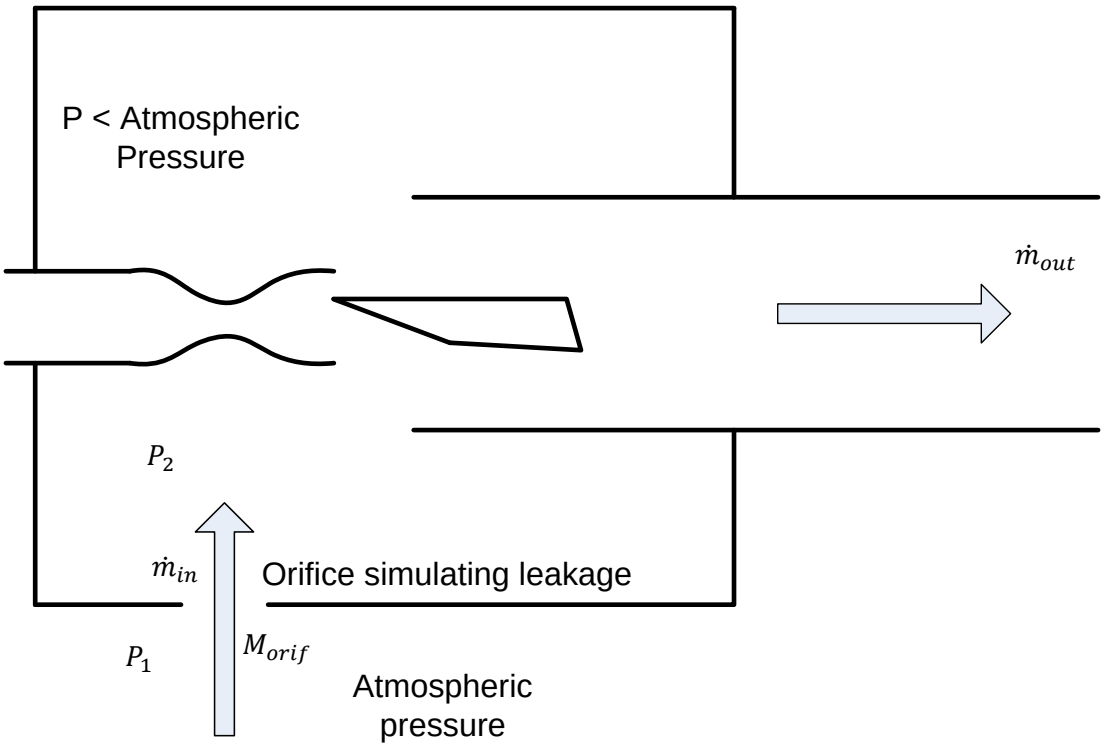

Figure 7: Test Cell Control Volume

Mass flow through an orifice and the resulting static pressure of the test cell are calculated using the following equations [20]:

$$M_{orif} = \sqrt{\frac{\left(\frac{P_2}{P_1}\right)^{\frac{2}{\gamma_1}} - \left(\frac{P_2}{P_1}\right)^{\frac{\gamma_1+1}{\gamma_1}}}{\frac{\gamma_1 - 1}{2}\left(\frac{2}{\gamma_1 + 1}\right)^{\frac{\gamma_1+1}{\gamma_1-1}}}} \tag{1}$$

$$\dot{m}_{in} = c_f M_{orif} A_{orif} P_1 \gamma_1 \left(\frac{2}{\gamma_1 + 1}\right)^{\frac{\gamma_1+1}{2(\gamma_1+1)}} \sqrt{\frac{g_c}{\gamma_1 R T_1}} \tag{2}$$

$P_1, \gamma_1 : atmospheric\ static\ press. and\ specific\ heat\ ratio;\ \ P_2 : test\ cell\ static\ press.$

$$m_{system} = m_{initial} + \int (\dot{m}_{in} - \dot{m}_{out})dt \tag{3}$$

$$P_{system} = (\rho RT)_{system} = \left(\frac{m}{V}RT\right)_{system} \tag{4}$$

Another important aspect of the ejector diffuser model is the mixing of the different flows (test cell secondary, free jet nozzle, test article, and ejector flow) as they meet in the diffuser. This is handled in a one dimensional sense by mixing properties of the different flows using the following equations:

$$c_{p1} = \frac{R_1\gamma_1}{\gamma_1 - 1}, c_{p2} = \frac{R_2\gamma_2}{\gamma_2 - 1} \tag{5}$$

$$c_{pmix} = \frac{c_{p1}\dot{m}_1 + c_{p2}\dot{m}_2}{\dot{m}_{mix}} \tag{6}$$

$$T_{tmix} = \frac{\dot{m}_1 c_{p1} T_{t1} + \dot{m}_2 c_{p2} T_{t2}}{c_{pmix}\dot{m}_{mix}} \tag{7}$$

$$R_{mix} = \frac{R_1\dot{m}_1 + R_2\dot{m}_2}{\dot{m}_{mix}} \tag{8}$$

$$\gamma_{mix} = \frac{1}{1 - \frac{R_{mix}}{c_{pmix}}} \tag{9}$$

This is done at each interface of two separate streams, and the new properties are used to make calculations with the appropriate air properties.

The model handles calculating a static pressure at certain locations by calculating and summing impulse functions (stream thrust) on the system. The Impulse Function, I, is defined as:

$$I = PA + \frac{\dot{m}v}{g_c} \tag{10}$$

Using the one dimensional mass flow equation ($\dot{m} = \rho A v$) and equation for a calorically perfect gas, the impulse function can be rewritten as:

$$F = I = PA(1 + \gamma M^2) \tag{11}$$

In this paper, it will be referred to as simply the force of the flow, F. Calculating the forces using the previous equation and summing them, the static pressure is then calculated. Shown below is the derivation and equations used to calculate this pressure:

Ideal gas properties:

$$P = \rho RT \tag{12}$$

$$a = \sqrt{\gamma RT g_c} \tag{13}$$

mass flow:

$$v = Ma \tag{14}$$

$$T = \frac{T_t}{1 + \frac{\gamma - 1}{2} M^2} \tag{15}$$

$$\dot{m} = \rho A v = \rho A M a = \rho A M \sqrt{\gamma R T g_c} = P A M \sqrt{\frac{\gamma g_c}{RT}} = P A M \sqrt{\frac{\gamma g_c}{R T_t}\left(1 + \frac{\gamma - 1}{2} M^2\right)} \tag{16}$$

rearranging the previous equation:

$$P = \frac{\dot{m}}{M A \left(\frac{\gamma g_c}{R T_t}(1 + \frac{\gamma - 1}{2} M^2\right)^{1/2}} \tag{17}$$

Pressure equation rearranged from previous Impulse equation:

$$P = \frac{F}{A(1 + \gamma M^2)} \tag{18}$$

Setting the previous two equations equal to each other and squaring both sides:

$$\frac{F^2}{A^2(1 + \gamma M^2)^2} = \frac{\dot{m}^2}{M^2 A^2 \left(\frac{\gamma g_c}{R T_t}\right)\left(1 + \frac{\gamma - 1}{2} M^2\right)} \tag{19}$$

Rearranging:

$$\left(g_c F^2 \left(\frac{\gamma^2 - \gamma}{2}\right) + \gamma^2(-\dot{m}^2 R T_t)\right) M^4 + (g_c F^2 \gamma - 2\gamma \dot{m}^2 R T_t) M^2 - \dot{m}^2 R T_t = 0 \tag{20}$$

Setting $C = -\dot{m}^2 R T_t$, $A = \left(g_c F^2 \left(\frac{\gamma^2 - \gamma}{2}\right) + \gamma^2(-\dot{m}^2 R T_t)\right)$ and $B = (g_c F^2 \gamma - 2\gamma \dot{m}^2 R T_t)$

and solving with the quadratic formula:

$$M^2 = \frac{-B \pm \sqrt{B^2 - 4AC}}{2A}, \quad \begin{matrix} -\ Supersonic\ Solution \\ +\ Subsonic\ Solution \end{matrix} \tag{21}$$

The static pressure can then be found using the rearranged impulse equation:

$$P = \frac{F}{A(1 + \gamma M^2)} \tag{22}$$

The model also has to calculate static conditions given total pressure, temperature, mass flow, and flow area. This is accomplished by converging on a Mach number using the following equation [11]:

$$M - \frac{\dot{m}}{AP_t\sqrt{\frac{\gamma g_c}{RT_t}}}\left(1 + \frac{\gamma - 1}{2}M^2\right)^{\frac{\gamma+1}{2(\gamma-1)}} = 0 \tag{23}$$

Subsonic Solution: Initial values for M = 0.0001, 1

Supersonic Solution: Initial values for M = 1, 10

These equations are iterated until a converged solution is obtained.

Static pressure and temperature can then be found using:

$$P = \frac{P_t}{\left(1 + \frac{\gamma - 1}{2}M^2\right)^{\frac{\gamma}{\gamma-1}}} \tag{24}$$

$$T = \frac{T_t}{1 + \frac{\gamma - 1}{2}M^2} \tag{25}$$

5.2.2 FREE JET NOZZLE & SECONDARY FLOW SUBSYSTEM

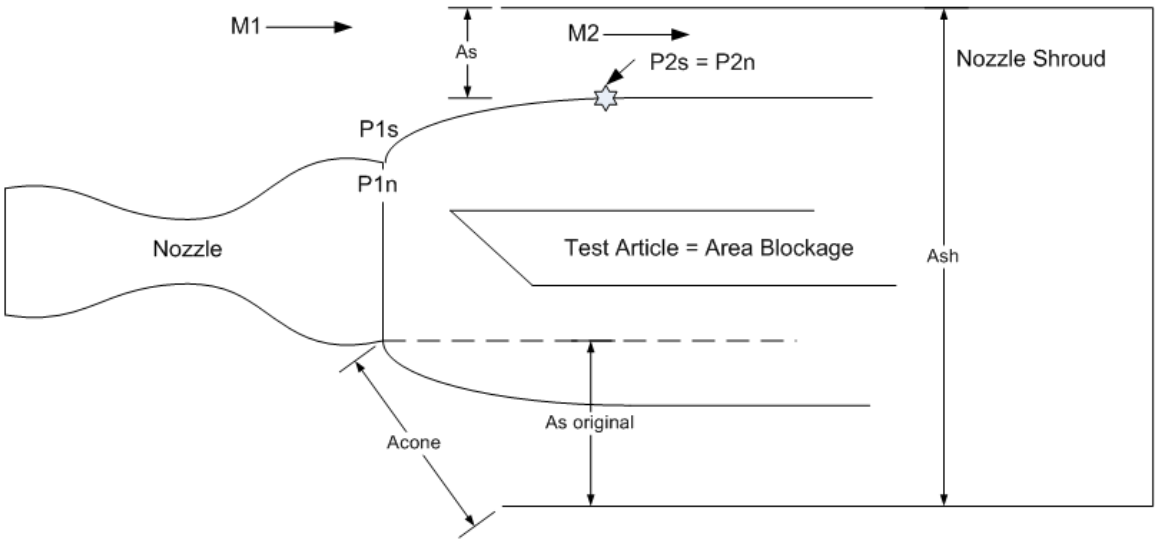

Figure 8: Free-jet Nozzle & Secondary Flow Diagram

The free-jet nozzle and the secondary airflow from the test cell make up the main subsystem in the ejector diffuser model. Due to the high temperatures and low pressures, all flows here are approximated here as an ideal gas. Figure 8 shows a simplified diagram of this subsystem. The computer model takes the static pressure at the exit of the nozzle and the test cell, P1n & P1s respectively, and calculates an area for the secondary flow at a choked condition. The derivation for this assumes that both flows are separate (no mixing occurs), the secondary flow Mach number at sta. 1 is ~0 to 0.1, the secondary flow is choked at sta. 2, and both flows expand/contract isentropically. In reality, the main cause of entrainment of the secondary flow is due to boundary layer mixing, but a fair approximation is to assume both flows as separate. The calculation works by finding a point in the flows (sta. 2) in which the static pressure of the nozzle

flow is equal to the static pressure of the secondary flow. At this point, no further contraction or expansion will take place downstream. If the nozzle exit static pressure is higher than the test cell static pressure, then the nozzle flow will expand out and thus constrict the secondary flow. If the conical flow area, Acone, is greater than the shroud area, Ash, minus the area blockage, then the choke point will occur at station 2 whether the nozzle flow expands or contracts. However, if the choked secondary flow area could be larger than the conical area, then the choking would occur at the smallest of the two areas. The following shows the derivation for the choked secondary flow area:

Isentropic expansion/contraction for secondary flow:

$$P_2 = P_{1s} \Bigg/ \left[\frac{1+\frac{\gamma-1}{2}M_2^2}{1+\frac{\gamma-1}{2}M_1^2}\right]^{\frac{\gamma}{\gamma-1}} \tag{26}$$

Isentropic expansion/contraction for nozzle flow:

$$P_2 = P_{1n}\left(\frac{V_1}{V_2}\right)^{\gamma} = P_{1n}\left(\frac{A_1(1)}{A_2(1)}\right)^{\gamma} = P_{1n}\left(\frac{A_{noz}}{A_{sh}-A_s}\right)^{\gamma} \tag{27}$$

Setting the two equations equal to each other:

$$P_{1n}\left(\frac{A_{noz}}{A_{sh}-A_s}\right)^{\gamma} = P_{1s} \Bigg/ \left[\frac{1+\frac{\gamma-1}{2}M_2^2}{1+\frac{\gamma-1}{2}M_1^2}\right]^{\frac{\gamma}{\gamma-1}} \tag{28}$$

And finally solving for secondary airflow area, As, results in:

$$A_s = A_{sh} - \frac{A_{noz}}{\left[\frac{P_{1s}}{P_{1n}} \Big/ \left[\frac{1+\frac{\gamma-1}{2}M_2^2}{1+\frac{\gamma-1}{2}M_1^2}\right]^{\frac{\gamma}{\gamma-1}}\right]^{\frac{1}{\gamma}}} - A_{blockage} \tag{29}$$

The area blockage term is an input of the estimated effective blockage due to the test article and thrust stand. This would be the effective area of the test article and thrust stand minus the inlet area perpendicular to the flow. This effective area includes the boundary layer effects such that a blunt body would have a larger effective area than a streamlined body. After the choked secondary flow area is calculated, the corresponding choked mass flow can be calculated with the following equations:

$$T_2 = \frac{T_1}{\left[\frac{1+\frac{\gamma-1}{2}M_2^2}{1+\frac{\gamma-1}{2}M_1^2}\right]}, M_1 = 0,\ M_2 = 1.0 \tag{30}$$

$$a_2 = \sqrt{\gamma R T_2 g_c} \tag{31}$$

$$\rho_2 = \frac{P_2}{R T_2} \tag{32}$$

$$\dot{m}_s = \rho_2 A_s a_2 \tag{33}$$

$$F_s = P_2 A_s (1+\gamma) \tag{34}$$

The mass flow calculated above is the limiting condition for the free-jet nozzle & secondary flow subsystem. It is the maximum amount of airflow from the test cell possible given the conditions at that point in time. This maximum flow and

corresponding force is summed with the free-jet nozzle flow, and ejector flow to calculate a diffuser exit static pressure. If this calculated pressure is greater than or equal to the pressure that the diffuser dumps to (atmospheric pressure in the model), then the model uses this as its secondary airflow. If the calculated diffuser exit pressure is less than atmospheric pressure, then the model iterates between the negative and positive value of this max airflow until the diffuser exit static pressure equals the pressure to which the diffuser is dumping. The following chart (Figure 9) illustrates why this calculation method works:

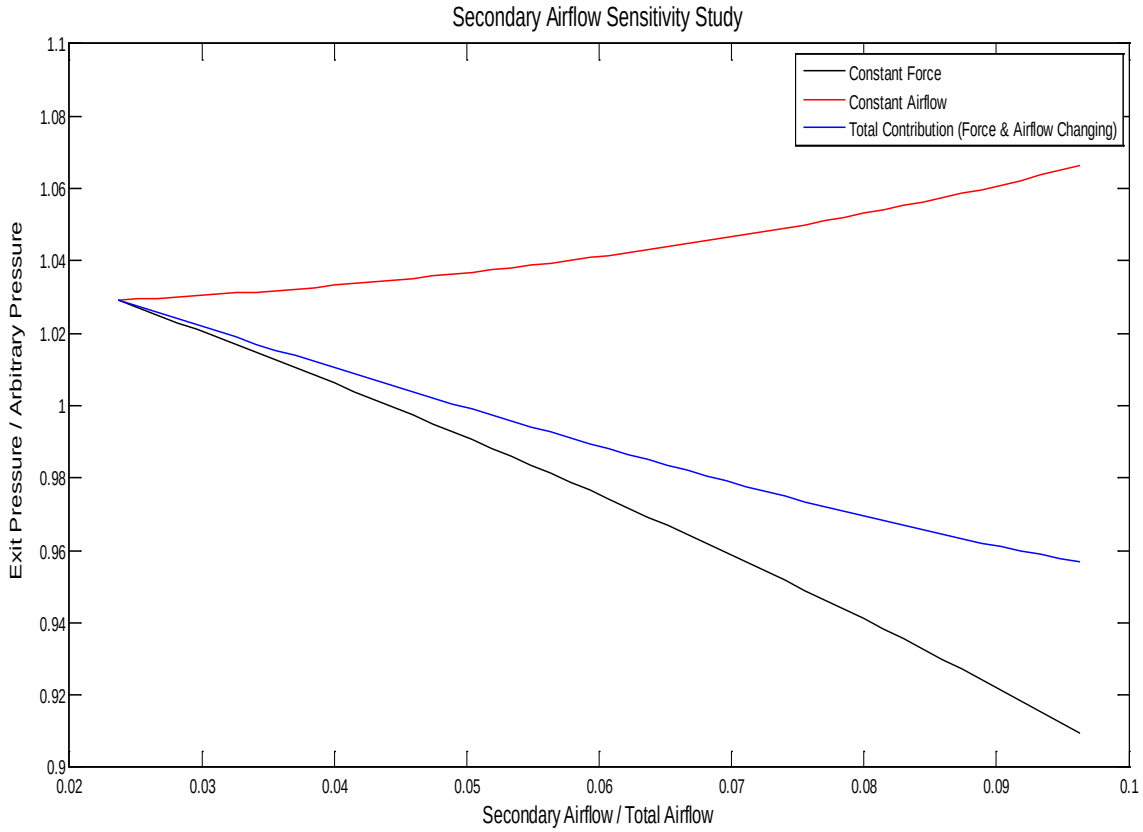

Figure 9: Secondary Airflow Sensitivity

As the figure above illustrates, increasing secondary airflow does two opposing things which affect the exit pressure. As secondary airflow increases, the force of this flow increases as well. Increasing mass flow while holding the force of the flow constant shows that the exit pressure increases. Increasing the force of the flow while holding the mass flow constant shows that the exit pressure decreases at a faster rate. So the total contribution of increasing the secondary airflow is to decrease the static exit pressure. Essentially, if the diffuser exit pressure calculated with maximum secondary airflow is less than the diffuser dumping pressure, then this secondary airflow must be reduced to increase the exit diffuser pressure. The iteration calculation method used is as follows:

1) Calculate choked secondary flow area & corresponding force (eqns. 29-34)
2) Mix properties of nozzle, secondary, and ejector flows (eqns. 5-9)
3) Sum forces and mass flow rates from all flows (free-jet nozzle, secondary flow, ejectors, test article)
4) Given flow area, Mach number, total temp., total force, and flow properties at diffuser exit, calculate a static pressure using the method shown previously. The subsonic solution essentially calculates the static pressure at the diffuser exit equivalent to the pressure drop across a normal shock. (eqns. 20-22)
5) This calculated diffuser exit static pressure, P4, is multiplied by a correction factor of ~0.8 (specifically 0.78 for diffuser modeled) as shown in Fig. 4. This correction factor corrects for the difference in a normal shock pressure

loss and what actually occurs in a real diffuser (complex system of normal and/or oblique shocks)

6) If P4 > Patm, then calculate limiting condition for ejector diffuser flow (shown later) and take choked secondary airflow (Wsmax) as actual airflow and exit routine

7) If P4 < Patm, then set Wsa = - Wsmax , Wsb = +Wsmax, Ws = 0.5*(Wsa+Wsb)

8) Calculate secondary airflow static pressure (Ps1), static temperature, & Mach number given total pressure, total temperature, Ws, As, and air properties using (eqns. 23-25). Then a new secondary airflow force (Fs) is calculated with the following equation:

$$F_s = P_{s1} A_s (1 + \gamma) \tag{35}$$

9) Mix properties of nozzle, secondary, and ejector flows

10) Given flow area, Mach number, total temp., total force, and flow properties at diffuser exit, calculate a static pressure (P4) using the method shown previously.

11) Calculate the difference between calculated P4 & Patm and the difference between Wsa & Wsb. If pressure difference is less than 0.01 or airflow difference is less than 0.1, then secondary airflow solution has converged. Then the limiting ejector diffuser condition is calculated (shown later) and routine ends.

12) If solution has not converged, then new Wsa, Wsb, & Ws are calculated using the bisection method. Then steps 8 through 12 are repeated.

5.2.3 EJECTOR NOZZLES & EJECTOR SECONDARY FLOW SUBSYSTEM

Downstream of the free-jet nozzle and test article is the ejector system which works to further entrain the combined upstream flow through the diffuser. It does this through boundary layer mixing but is modeled as two separate streams here (combined free-jet nozzle with test cell secondary flow and the ejector flow). This subsystem can in effect be modeled in the same way as the free-jet nozzle & secondary flow subsystem. However, one additional complication to this problem is with the ejector flows. The following graph shows arbitrary values of a typical high pressure ejector nozzle system.

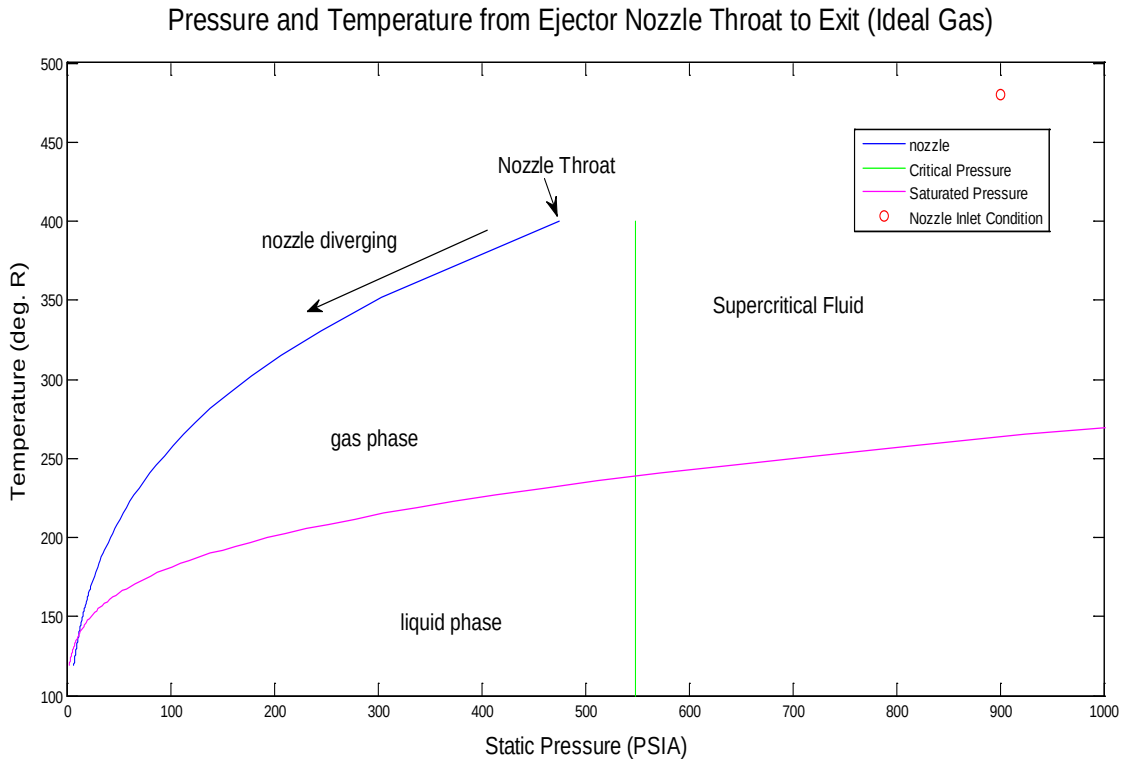

Figure 10: Typical High Pressure Ejector Nozzle Flow Phase Diagram

As shown in figure 10, as the air passes through the divergent section of the ejector nozzle, the flow is rapidly cooled and crosses over the liquid phase line near the exit. In reality, once it nears the liquid phase line, some condensation would occur but this would increase the heat transfer rate thus keeping it from turning to all liquid. However, due to the fact that this model doesn't account for heat transfer from the air to the nozzle, the temperature at the exit will probably be higher than what is shown thus raising it above the liquid phase line. Also, even with heat transfer not accounted for, the resulting nozzle exit pressure and temperature is very close to where it would be if it trailed the top border of the liquid phase region. Due to this fact, it is reasonable that the model does not account for this possibility of entering the liquid phase.

Another concern for the high pressures and low temperatures that would be common for the ejector nozzles is the ideal gas assumption. At these conditions, a significant error in mass flow at the nozzle throat can occur when using the ideal gas assumption. This will also affect the net force of the flow due to the differences in mass flow and air properties at the exit. The model has incorporated a switch that allows it to be switched from either calculating this mass flow and force with the ideal gas assumption or using pseudo real gas relations. The algorithm uses a real gas subroutine that calculates real gas density, sonic velocity, specific heat ratio, and compressibility factors using virial coefficients of air.

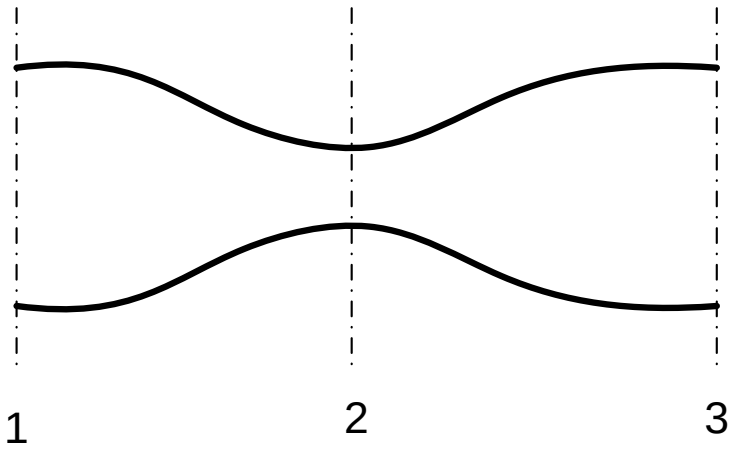

Figure 11: Nozzle Station Nomenclature

The steps of the algorithm are shown below (see Figure 11 for nomenclature):

1) Nozzle inlet temperature and pressure are input into the real gas subroutine and a real gas specific heat ratio ($\gamma_{inletRG}$) is calculated
2) Specific heat ratio found in step 1 is used to calculate a real gas temp. & pressure at the throat using the following equations [11]:

$$T_2 = \frac{2T_1}{\left(\gamma_{1\_RG} + 1\right)} \tag{36}$$

$$P_2 = \frac{P_1}{\left[1 + \frac{\left(\gamma_{1\_RG} - 1\right)}{2}\right]^{\frac{\gamma_{1\_RG}}{\left(\gamma_{1\_RG} - 1\right)}}} \tag{37}$$

3) P_2 and T_2 are input into the real gas subroutine, and a real gas density and sonic velocity are calculated at the throat.

4) Real gas mass flow is calculated using throat area, density, and sonic velocity using the following equation:

$$\dot{m}_{RG} = \rho_{2\_RG} A_2 a_{2\_RG} \tag{38}$$

5) It is assumed that at the ejector nozzle exit, the gas is ideal and its specific heat ratio is ~1.4 so an average specific heat ratio from throat to the exit is calculated by:

$$\gamma_{avg} = \frac{\left(1.4 + \gamma_{2\_RG}\right)}{2} \tag{39}$$

6) A new throat area is calculated using this average specific heat ratio (γ_{avg}) with the following ideal gas equation:

$$A_2 = \frac{\dot{m}_{RG}}{P_1 \sqrt{\frac{\gamma_{avg} g_c}{R_1 T_1} \left(\frac{\gamma_{avg} + 1}{2}\right)^{\frac{(\gamma_{avg}+1)}{(1-\gamma_{avg})}}}} \tag{40}$$

7) The nozzle inlet temp., pressure, modified throat area (A_2), and average throat to exit specific heat ratio (γ_{avg}) are input into an ideal gas nozzle subroutine that calculates the exit nozzle force, mass flow, exit pressure, exit temp., and exit Mach number.

The ideal gas nozzle [7] subroutine is a simple routine that uses the following equations:

choked flow through throat:

$$\dot{m} = P_{t1} A_2 \sqrt{\left(\frac{\gamma_1 g_c}{R_1 T_{t1}}\right)\left(\frac{\gamma_1 + 1}{2}\right)^{\frac{\gamma_1+1}{-(\gamma_1-1)}}} \tag{41}$$

initial Mach # estimate:

$$AR = \frac{A_3}{A_2} \tag{42}$$

$$M_3 = 1 + \gamma_1 \ln(AR) \tag{43}$$

converging on a Mach number:

$$M_1 = \frac{2 + (\gamma_1 - 1){M_3}^2}{\gamma_1 + 1} \tag{44}$$

$$M_2 = \sqrt{M_1^{\frac{\gamma_1+1}{\gamma_1-1}}} \tag{45}$$

$$\Delta AR = \frac{M_2}{M_3} - AR \tag{46}$$

$$\frac{\Delta AR}{\Delta M_3} = \left(\frac{1}{M_1} - \frac{1}{M_3^2}\right) M_2 \tag{47}$$

$$M_3 = M_3 - \Delta AR \Big/ \frac{\Delta AR}{\Delta M} \tag{48}$$

iterate until $\frac{\Delta AR}{AR}(100) \leq 0.01$

exit conditions:

$$P_3 = P_1\left(1 + \frac{\gamma_1 - 1}{2} M_3^2\right)^{\frac{\gamma_1}{1-\gamma_1}} \tag{49}$$

$$F_3 = P_3 A_3 (1 + \gamma_1 M_3^2) \tag{50}$$

$$T_{t3} = T_1\left(1 + \frac{\gamma_1 - 1}{2} M_3^2\right) \tag{51}$$

It is worth noting that other effects which could be as large as real gas effects, such as viscous boundary layer effects, were not included. These could be improvements worth adding to the model in the future.

As mentioned previously, besides the real gas complication with the ejector flow, the ejector nozzle & ejector secondary flow subsystem can be modeled in the similar fashion as the free jet nozzle & secondary flow subsystem. Figure 12 below is a simple schematic of the ejector diffuser system.

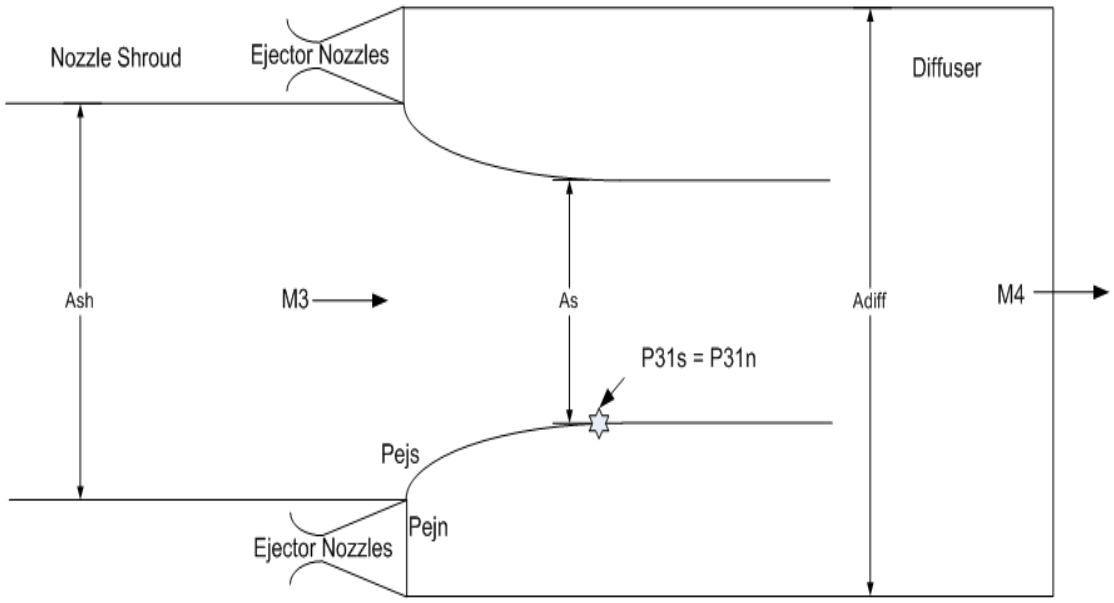

Figure 12: Ejector Nozzles & Ejector Secondary Flow Diagram

The main equations used to calculate the secondary flow area (As) and the resulting choked mass flow at sta. 31 are the following:

$$M_3 = \sqrt{\frac{F_3}{P_3 A_{sh} \gamma_3}} \tag{52}$$

$$A_s = A_{diff} - \frac{A_{ej}}{\frac{P_{ej}}{P_3} \Big/ \left[\frac{1 + \frac{\gamma_3 - 1}{2}}{1 + \frac{\gamma_3 - 1}{2} M_3^2}\right]^{\frac{1}{\gamma_3}}} \tag{53}$$

$$\dot{m}_{31choked} = P_3 A_s \sqrt{\frac{\gamma_3 g_c \left(1 + \frac{\gamma_3 - 1}{2}\right)}{R_3 T_{t3}}} \left[\frac{1 + \frac{\gamma_3 - 1}{2} M_3^2}{1 + \frac{\gamma_3 - 1}{2}}\right]^{\frac{\gamma_3}{\gamma_3 - 1}} \tag{54}$$

The assumptions made here are the same as for the free-jet nozzle subsystem. Both flows are modeled as ideal gas undergoing an isentropic expansion/contraction and the flow at station 31 is choked (M = 1). The mass flow $\dot{m}_{31choked}$ is the limiting ejector diffuser condition that was mentioned in the previous free jet nozzle subsystem algorithm. It is the max flow that can be achieved through the diffuser at the given conditions. If the determined test cell secondary airflow summed with the free jet nozzle flow is greater than the maximum possible diffuser airflow ($\dot{m}_{31choked}$), then the test cell secondary airflow must be reduced, based on the following equations:

$$\dot{m}_{31choked} = \dot{m}_3 = \dot{m}_{freejetnozzle} + \dot{m}_{testcell} \tag{55}$$

$$\dot{m}_{testcell} = \dot{m}_{31choked} - \dot{m}_{freejetnozzle} \tag{56}$$

Otherwise, if the maximum diffuser airflow is greater than the airflow coming into the diffuser, then no changes are made to the secondary airflow.

5.2.4 TEST ARTICLE & THRUST STAND SUBSYSTEM

The third subsystem that has been modeled is the test article and thrust stand. The thrust stand and test article introduce a drag on the passing air. Also, when the test article is an engine (ram/scramjet), it produces thrust as well. For typical ram/scramjets, the drag and thrust components are small compared to the large forces of the free-jet nozzle and ejector system. For this reason, the test article had been excluded from the previous ejector diffuser model. However, for better accuracy, a simplified method was developed to estimate some of the effects of the test article and thrust stand. A parametric model of an ideal ramjet was implemented into the computer model to estimate the gross thrust when the ram/scramjet is on. Figure 13 illustrates the nomenclature used in the parametric analysis.

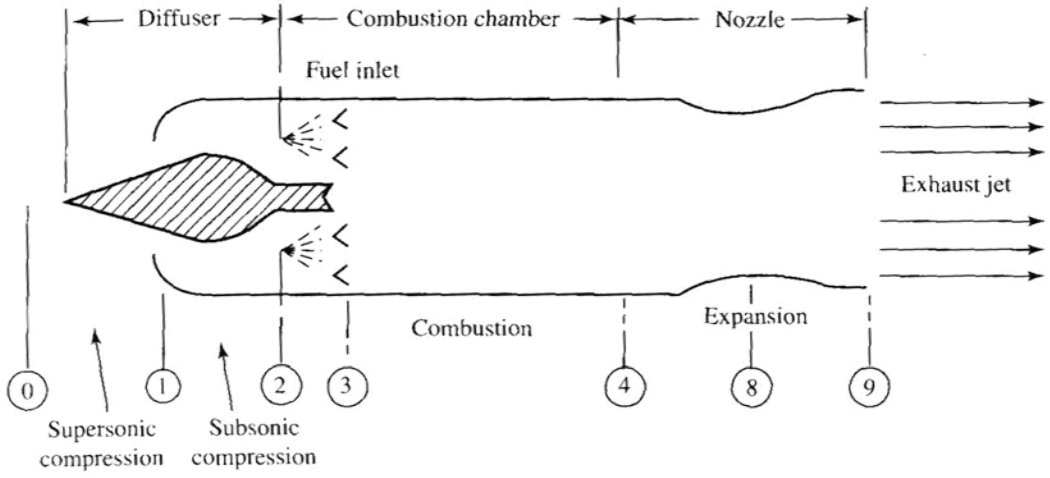

Figure 13: Ramjet Station Nomenclature [10]

The following is a summary of equations that were used [10].

$$a_0 = \sqrt{\gamma R g_c T_0} \tag{57}$$

$$\tau_r = \frac{T_{t0}}{T_0} = 1 + \frac{\gamma - 1}{2} M_0^2 \tag{58}$$

$$\tau_\lambda = \frac{T_{t4}}{T_0} \tag{59}$$

$$\frac{v_9}{a_0} = M_0 \sqrt{\frac{\tau_\lambda}{\tau_r}} \tag{60}$$

$$F_{NET} = \frac{\dot{m}_0 a_0}{g_c} \left(\frac{v_9}{a_0} - M_0 \right) \tag{61}$$

$$F_{GROSS} = \frac{\dot{m}_0 a_0}{g_c} \left(\frac{v_9}{a_0} \right) \tag{62}$$

$$\dot{m}_0 = \rho A_{inlet} M_0 a_0 \tag{63}$$

$$f = \frac{c_p T_0}{h_{pr}} (\tau_\lambda - \tau_r) \tag{64}$$

$$S = \frac{f}{F_{NET} / \dot{m}_0} \tag{65}$$

$$\eta_T = 1 - \frac{1}{\tau_r} \tag{66}$$

$$\eta_P = \frac{2}{\sqrt{\tau_\lambda / \tau_r} + 1} \tag{67}$$

$$\eta_O = \eta_T \eta_P \tag{68}$$

The assumptions used to develop these equations are:

$$P_9 = P_0 \tag{69}$$

$$\dot{m}_9 \cong \dot{m}_0 \tag{70}$$

$$\gamma_9 = \gamma_0 = \gamma \tag{71}$$

$$R_9 = R_0 = R \tag{72}$$

$$\frac{P_{t2}}{P_{t0}} = \frac{P_{t4}}{P_{t2}} = \frac{P_{t9}}{P_{t4}} = 1 \tag{73}$$

$$\frac{P_{t9}}{P_9} = \frac{P_0}{P_9}\frac{P_{t0}}{P_0}\frac{P_{t2}}{P_{t0}}\frac{P_{t4}}{P_{t2}}\frac{P_{t9}}{P_{t4}} = \frac{P_0}{P_9}\frac{P_{t0}}{P_0}(1)(1)(1) \tag{74}$$

The main inputs that go into this ram/scramjet model are the fuel lower heating value (h_{pr}), engine inlet area (A_{inlet}), and the operating total burner temperature (T_{t4}). This T_{t4} is the main control parameter for the engine operation, and the engine start is simulated by a ramp of T_{t4} to the operating temperature input into the model.

The previous parametric ramjet model only accounts for the gross thrust of the test article and not the drag. The net drag of the test article and the thrust stand can be significant while the engine is off. This occurs when the facility is ramping to the appropriate flight condition, as well as at the end of a test run. The approach used to model this drag allows the use of scale force data from prior projects to calculate a (drag coefficient*area) term for the test article and thrust stand as a single unit. Typical data

from a test run are Mach number, dynamic pressure, and the resulting engine off and on scale force at that condition. The equation for drag coefficient is:

$$c_d = \frac{D}{\rho A \, v^2/_2} \tag{75}$$

And the equation for dynamic pressure, Q, is:

$$Q = \frac{1}{2}\rho v^2 \tag{76}$$

Therefore, we can rearrange the drag coefficient equation to include Q.

$$c_d A = \frac{D}{\rho v^2/_2} = \frac{D}{Q} \tag{77}$$

Thus, the $c_d A$ term is simply the scale force of the thrust stand when the engine is off divided by the dynamic pressure. Then this number can be input into the model to calculate drag based on the simulated values of dynamic pressure.

$$D = (c_d A) \, \rho v^2/_2 = (c_d A) Q \tag{78}$$

Of course, this drag term does change based on Mach number and test article geometry, but it can be assumed approximately constant since the free-jet nozzle is modeled as a fixed geometry nozzle. Therefore, when on condition, the Mach number of the free-jet exit flow should remain fairly constant.

Several other options were put into the model that allow for different methods of calculating the effects of the test article and thrust stand. These were included to allow

for more flexibility in each simulation run. The additional options in this model are the following: using the $c_d A$ term to calculate drag and ramping this drag to zero once the engine starts (engine thrust ≈ drag); using the $c_d A$ term to calculate drag and ramping the engine gross thrust to a input constant. Figures 14 and 15 show diagrams of the Simulink model used for the test article.

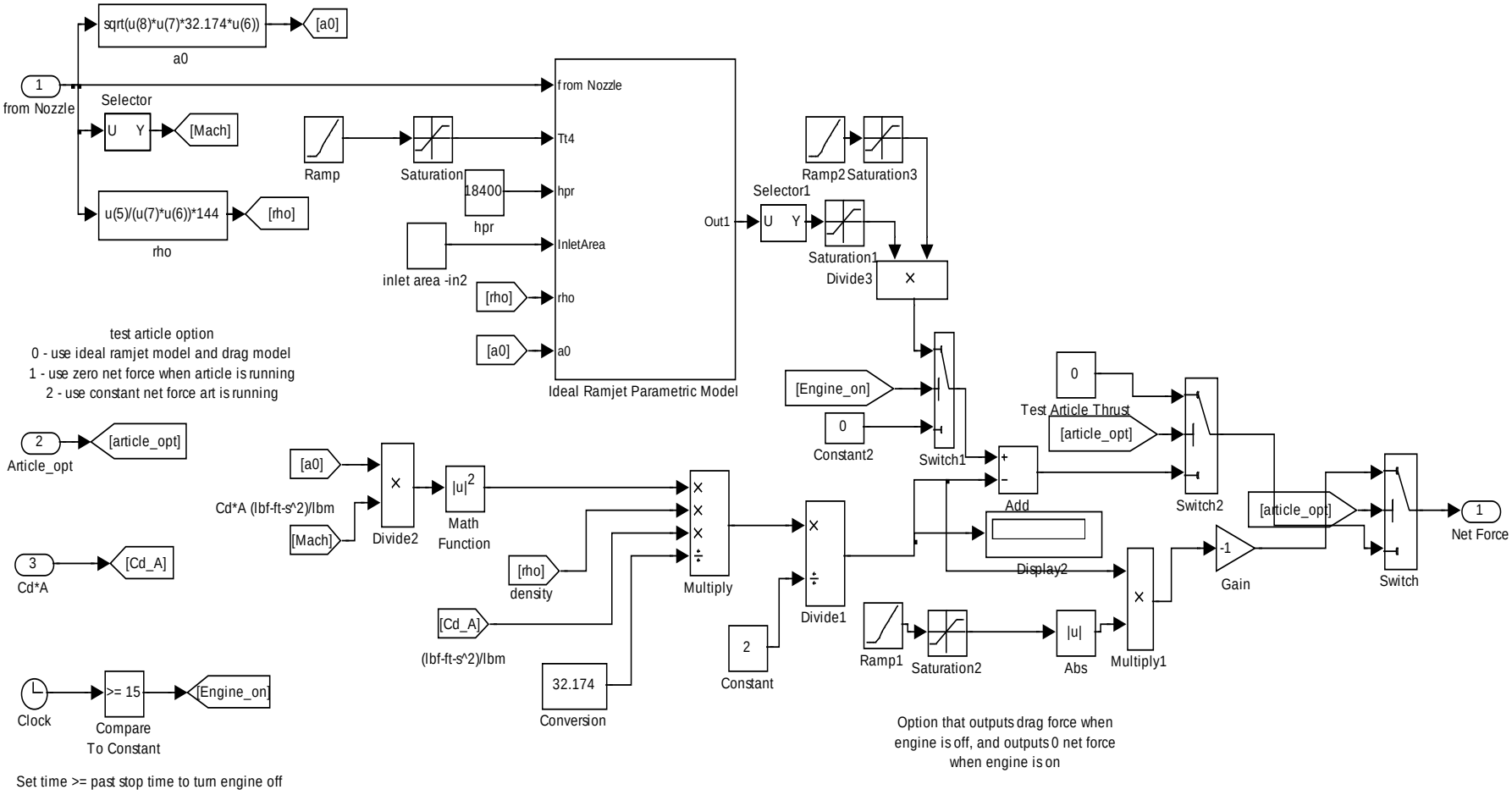

Figure 14: Test Article/Thrust Stand Simulink Model

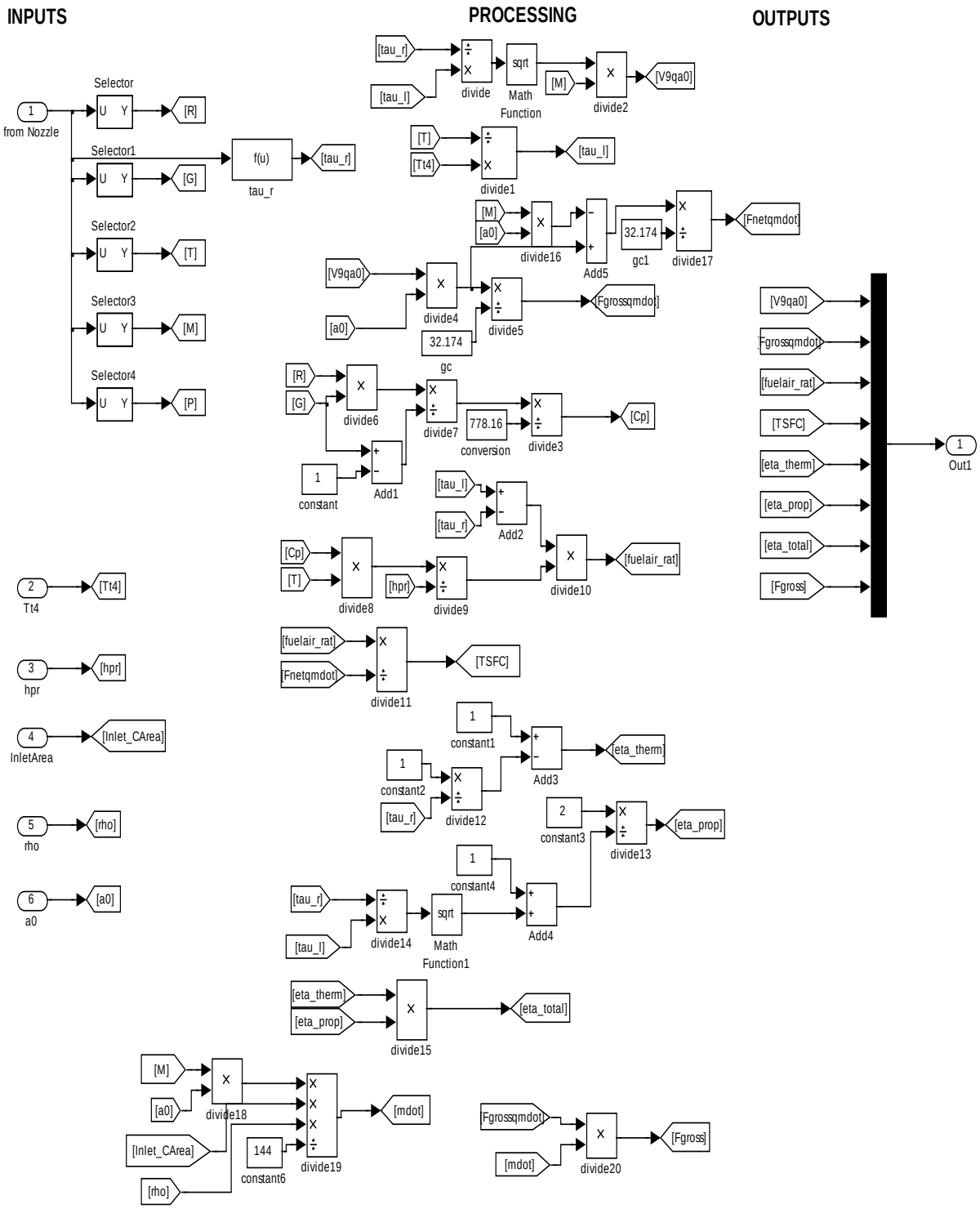

Figure 15: Ideal Ramjet Simulink Model

6. RESULTS

The new ejector diffuser system model better simulates the test cell pressure as it reacts to changes in the nozzle and ejector flows. The inclusion of the test article drag, thrust, and blockage shows improvements in matching experimental test data. Real gas calculations of the ejector flows also add additional accuracy to the model. One other major improvement is in calculating the constriction of the secondary airflows by either the free-jet nozzle or ejector nozzles. This enables the simulation of the started ejector mode of operation in which the test cell pressure becomes approximately a function of a constant pressure ratio (test cell static pressure / nozzle total pressure), and thus test cell pressure increases as the free-jet nozzle or ejector nozzle total pressure increases. It was already shown that the previous ejector diffuser model did not simulate this due to not calculating this constriction of the flow from the nozzle plume.

The data shown here in the results have been non-dimensionalized by dividing by the maximum pressure shown on the plot or an arbitrary common pressure when comparing one or more data sets. Several simulations were run with different modeling options set so that the contributions of various parts of the model can be seen. Shown below (Figure 16) is a simulation run that includes the following options: 1) Real Gas Ejector Flow; 2) Test Article/Thrust Stand Drag and Blockage Area; 3) Ideal Ramjet Test Article Gross Thrust Calculated. A nominal leakage term and flow coefficient were chosen for the test cell, and an estimate for test article inlet area, blockage area, cd*A term, operating Tt4 (burner total temp.), and fuel lower heating value were chosen for the ramjet model.

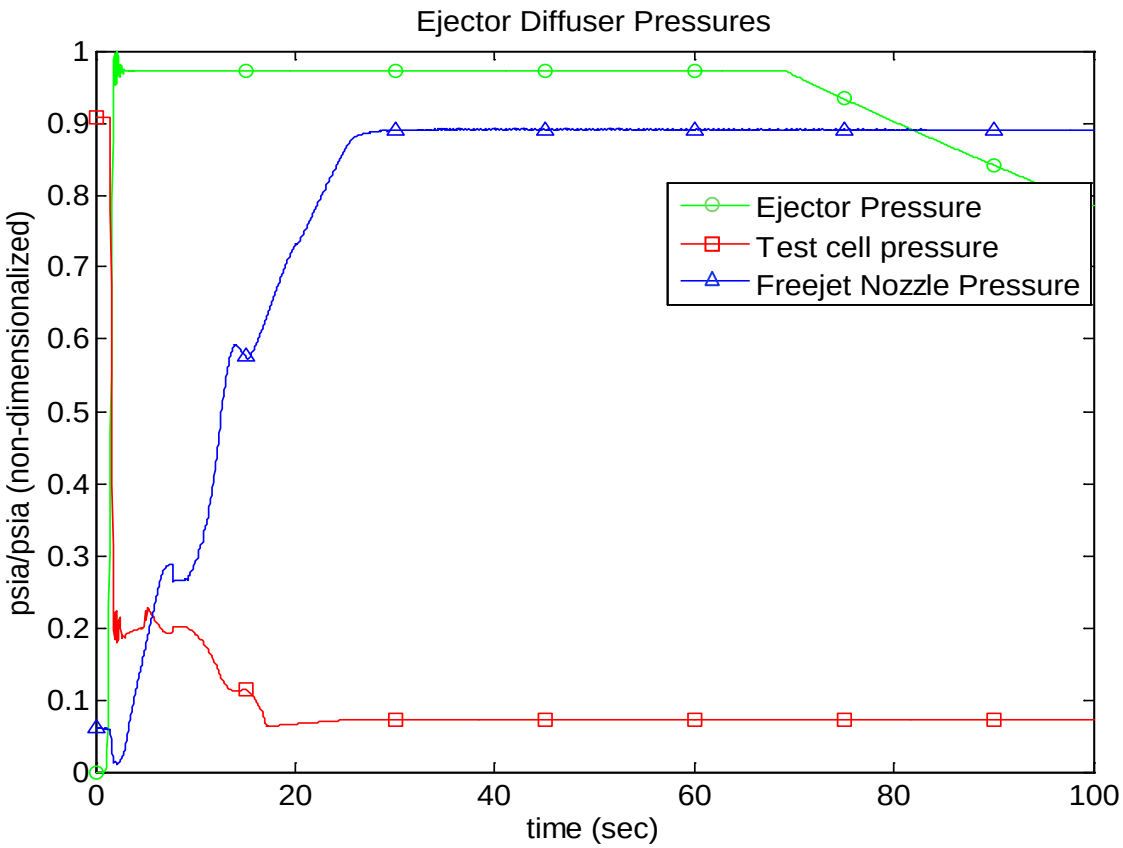

Figure 16: Ejector Diffuser Simulation Pressures with Ramjet Model

The interesting section of Figure 16 is prior to the ejector and free-jet nozzle pressures becoming a maximum value (prior to t = 30 sec.). This is when the driving pressures of the free-jet nozzle and ejector nozzles drive the test cell pressure to become constant (free-jet nozzle is started and secondary airflow from test cell is choked). Figure 17 shows the first 40 seconds of this simulation. Some oscillatory behavior can be seen in the test cell pressure at the beginning of the ejectors ramping to their operating pressure. This is due strictly to the oscillations of the ejector pressures which oscillate both the total force and mass flow of the system and thus drive test cell pressure to oscillate.

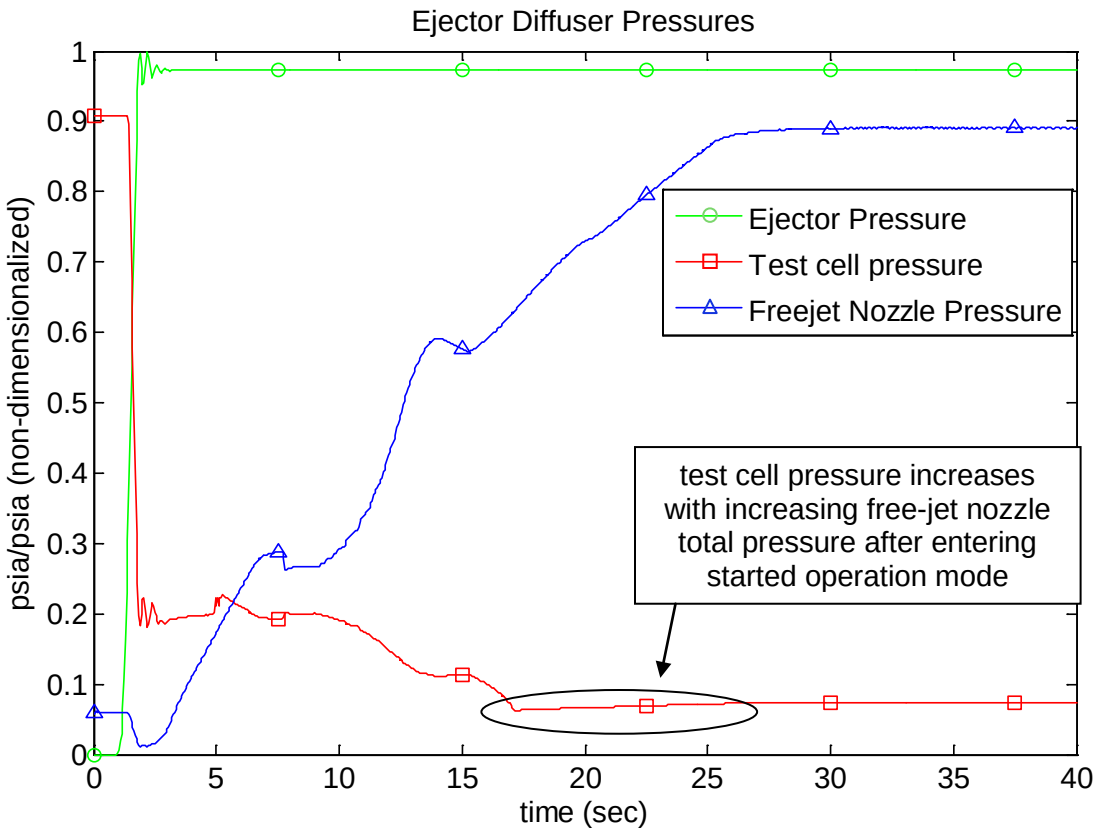

Figure 17: Detailed View-Ejector Diffuser Simulation Pressures with Ramjet Model

Damping of the system in reality would eliminate most of these oscillations in the ejector manifold pressure.

As was shown previously in Figure 3, ejector performance can be plotted as a ratio of the test cell pressure and diffuser exit pressure over the nozzle total pressure. In figure 18, we take a look at the ejector performance of the free-jet nozzle and how the test cell pressure/free-jet nozzle total pressure becomes approximately constant after it becomes started. This plot only looks at the time during which the ejector manifold pressure was constant (i.e. only the free-jet nozzle was further driving down test cell pressure).

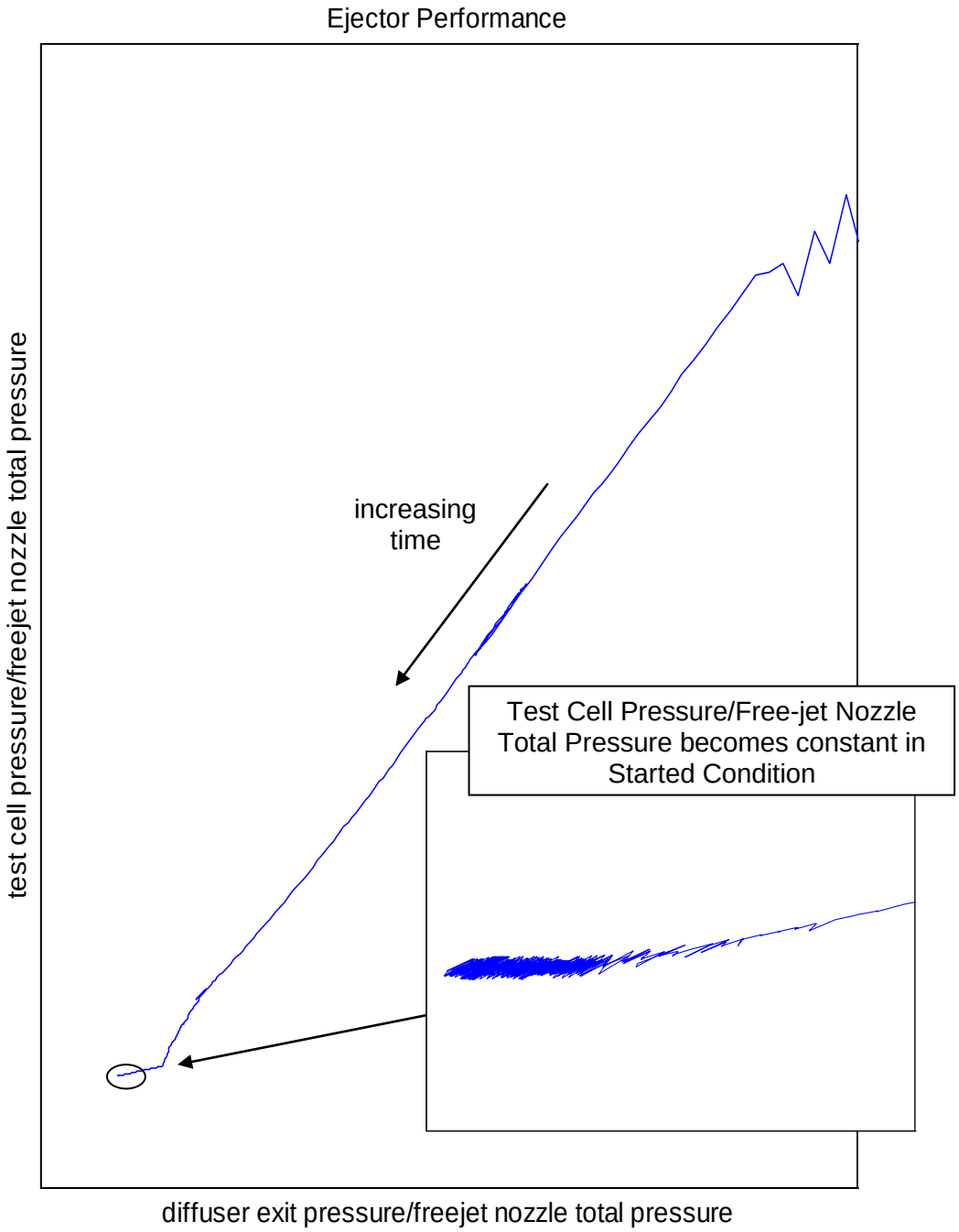

Figure 18: Simulation of Ejector Performance

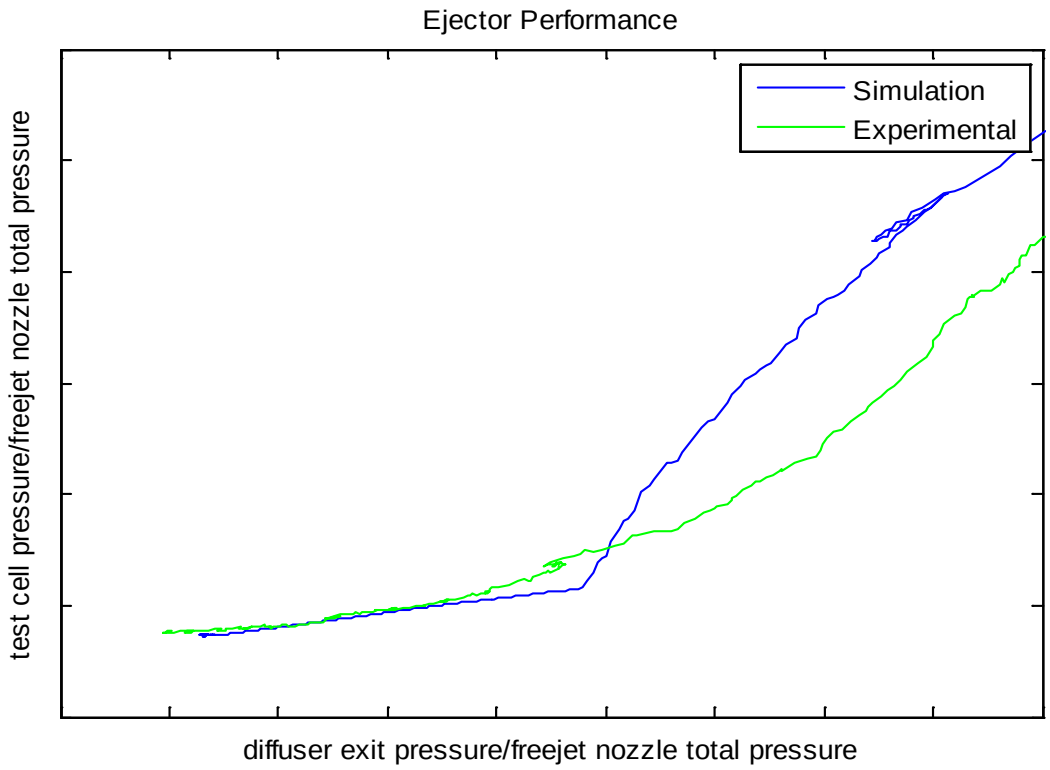

Figure 19: Detailed Ejector Performance Simulation vs. Experimental Comparison

Figure 19 shown above is a zoomed in view of Figure 18 and also shows the experimental data. As the plot shows, the final pressure ratio is very close to the model's.

Now, some results from the test article model will be shown. The full contribution of the test article is in the drag, thrust, and area blockage caused by the test article. As was noted before, the drag is calculated using a constant cd*A term derived from experimental data and the dynamic pressure calculated in the model. Finally, the gross thrust is calculated using a simple ideal ramjet model, and this term is subtracted by the drag term to get the net thrust on the system. The following chart, Figure 20, shows the non-dimensionalized contributions of these terms.

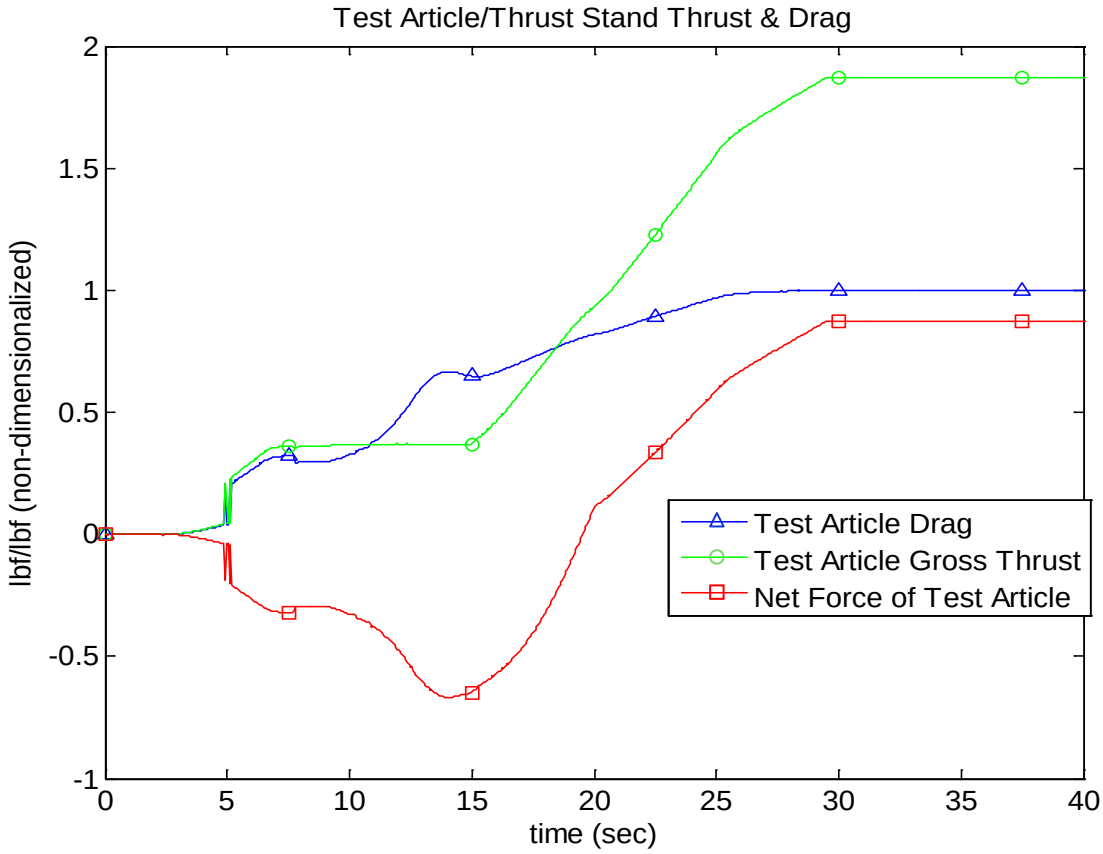

Figure 20: Test Article/Thrust Stand Thrust & Drag Simulation

The different options built into the new diffuser model allow the model to be tweaked to fit each problem more effectively. It also allows one to look at the contributions of the different options set. The next plot, Figure 21, shows two simulations, one with and one without test article thrust, drag, and area blockage. The other options set are the same for both simulations. In the simulation with the test article prior to t=20 sec, the test article net thrust was negative. Afterwards, the net thrust becomes positive.

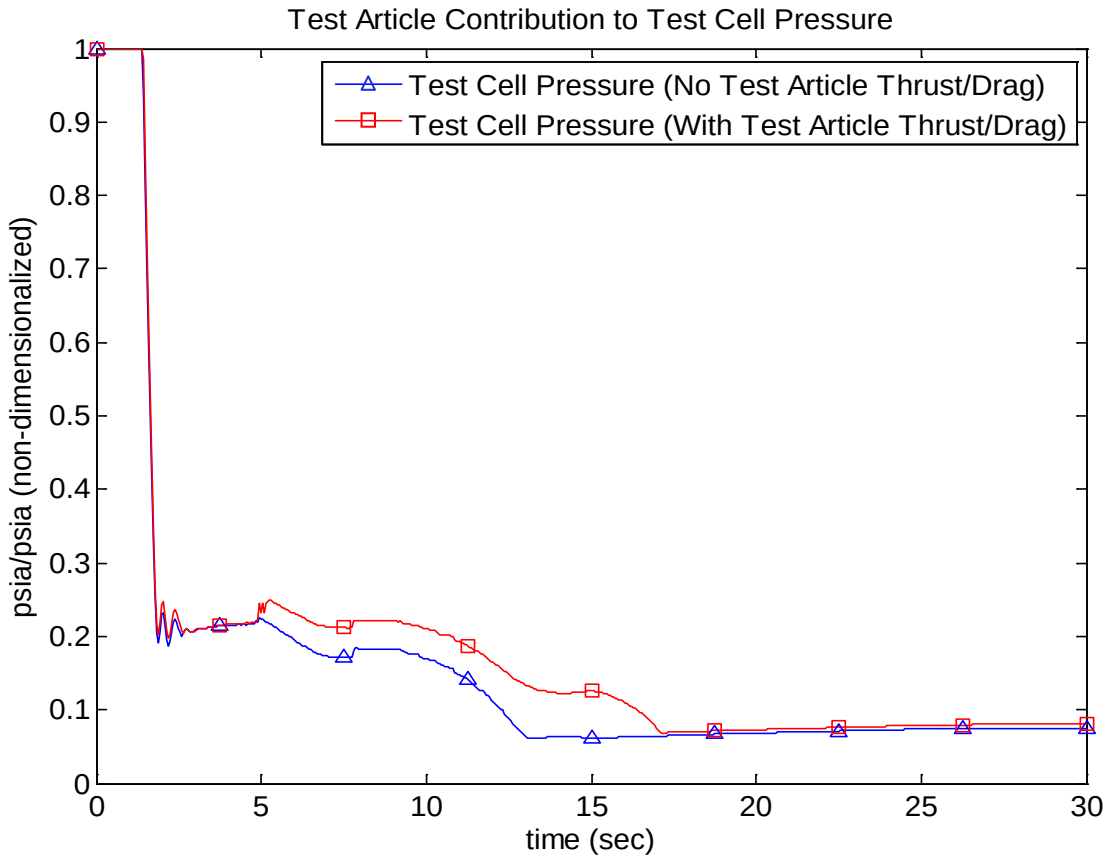

Figure 21: Test Article Contribution to Test Cell Pressure

A decrease in net thrust on the system results in less mass flow from the test cell needed to balance the pressure at the diffuser exit. Also, an area blockage will reduce the free-jet nozzle total pressure needed to choke the secondary flow from the test cell as well as reduce the choked flow area. This reduction in choked secondary flow area is the sole reason for the difference in the final test cell pressure attained. This plot shows that the inclusion of the test article results in both an increased final test cell pressure and a later onset of started flow. A similar plot shown below (Figure 22) simulates the case where the test article was in the test cell but not turned on. Thus, it's only effects are the drag and blockage area. This plot is very similar to Figure 21 but differs in that the test cell

pressure transition to constant pressure takes longer and is smoother. This is due to the test article net force being simply the drag and fairly constant as it enters a started mode. As noted previously, reductions in the net force of the system act to reduce secondary flow from the test cell thus increasing pressure. As can be seen on the previous two plots, the final test cell pressure was affected only by the addition of an effective blockage area term.

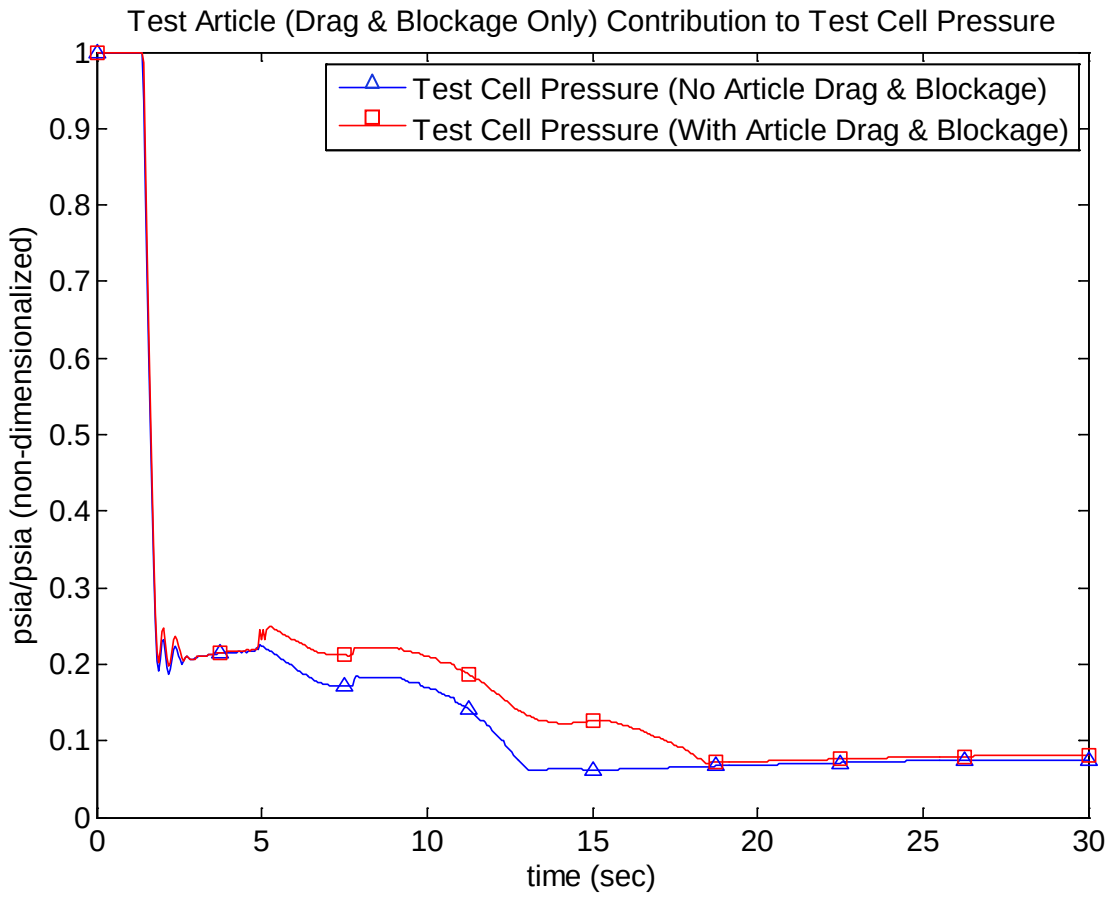

Figure 22: Test Article (Drag & Blockage Only) Contribution to Test Cell Pressure

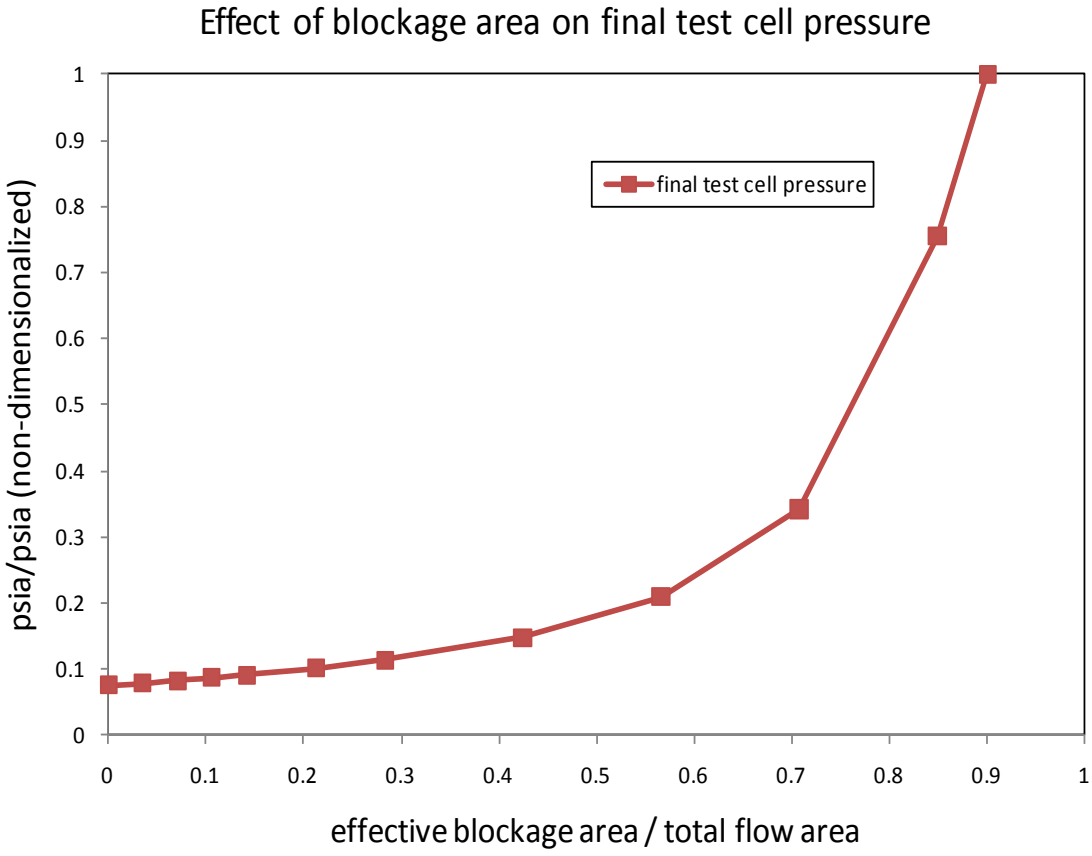

Figure 23: Effect of Blockage Area on Final Test Cell Pressure

Figure 23 illustrates the effect of different effective blockage areas on the final test cell pressure.

The real gas approach of calculating flow through the ejectors also has an effect on the system. Two more simulations were run to show the difference in calculating the ejector flows with ideal gas and real gas assumptions. The model was again setup as if the test article was not on (only drag and area blockage).

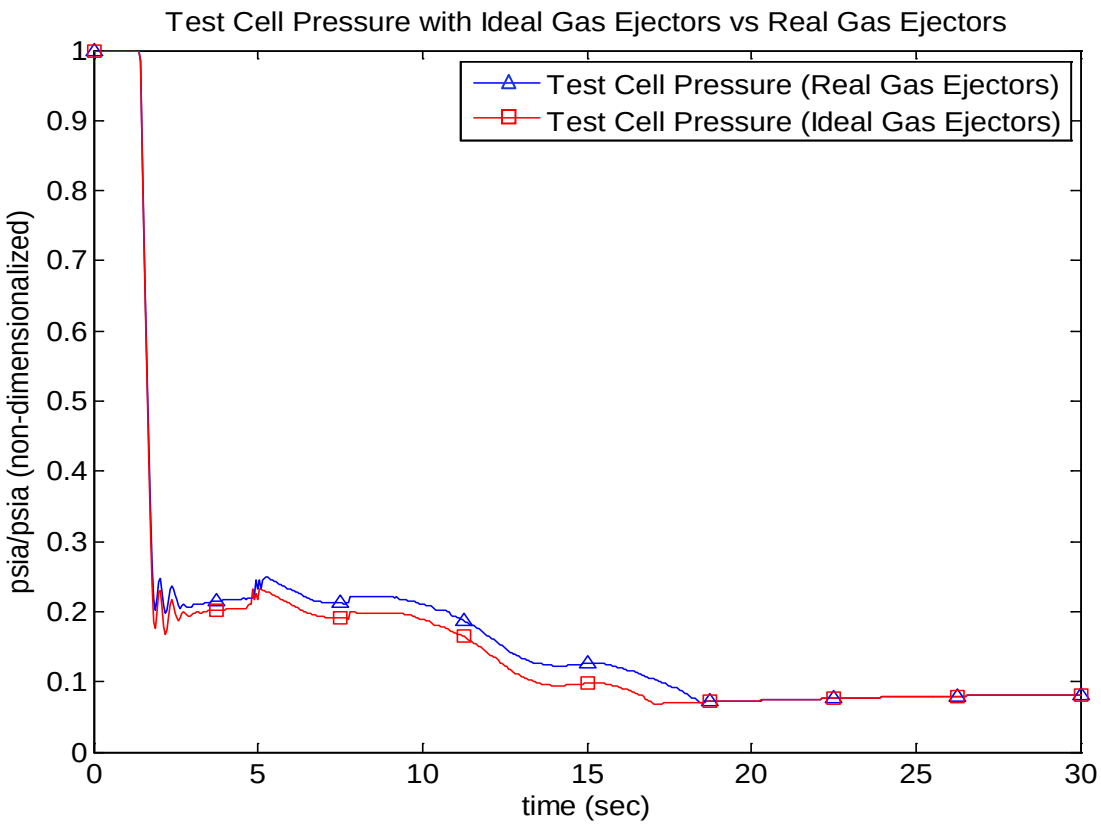

Figure 24: Test Cell Pressure with Ideal Gas vs. Real Gas Ejectors

The plot in Figure 24 shows that there is no difference in the final test cell pressure attained after the secondary airflow chokes. The real gas calculation of the ejector flows effectively increases the mass flow through the ejectors as compared to the ideal gas calculation. This results in a lower static pressure at the diffuser exit and thus a reduction in secondary airflow from the test cell. The final test cell pressure does not change because this depends only on the flow into the test cell (leakage) and the flow out of the test cell (through the diffuser). After the secondary flow is choked, the things that affect the final pressure are only the blockage area constricting the secondary flow and the leakage area and flow coefficient. Since the secondary flow area depends only on the

blockage area and the free-jet nozzle and test cell pressure, the final test cell pressure is identical for both simulations.

Experimental data for the simulated facility will be shown next. The data used is from a mass capture run in which the test article was in the test cell but not turned on. The drag (cd*A) term used in the facility model was derived using experimental data from the test article that is in the experimental mass capture run used here for comparisons (Figure 25). Due to the many differences in ramjet/scramjet performance, it was concluded that comparisons made using only the drag and blockage term of the test article would be more valid. Also, differences in the timing of the actual control system and the control system in the model result in the data being shifted on the time scale as shown in the following plot.

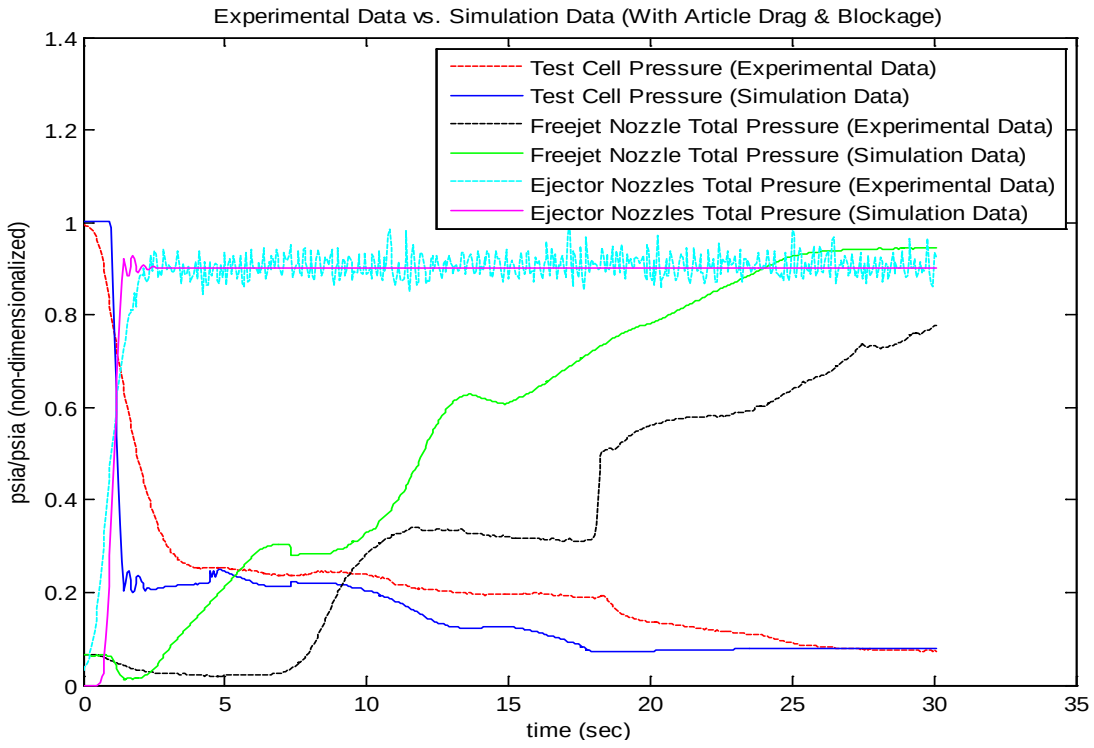

Figure 25: Experimental vs. Simulation Data (with Test Article Drag & Blockage)

This plot shows test cell pressure, free-jet nozzle total pressure, and ejector nozzles total pressure from both the simulation and the experimental data. A shift in the time scale for the simulation output is done to show the relationships of the two driving pressures (free-jet & ejectors) and the test cell pressure and how the simulation compares with the experiment. (Figure 26) As can be seen in this plot, the final test cell pressure is nearly identical for both the simulation and the experimental data (within 1 percent). Also, responses in the test cell pressures are very close for the same free-jet and ejector nozzle driving pressures.

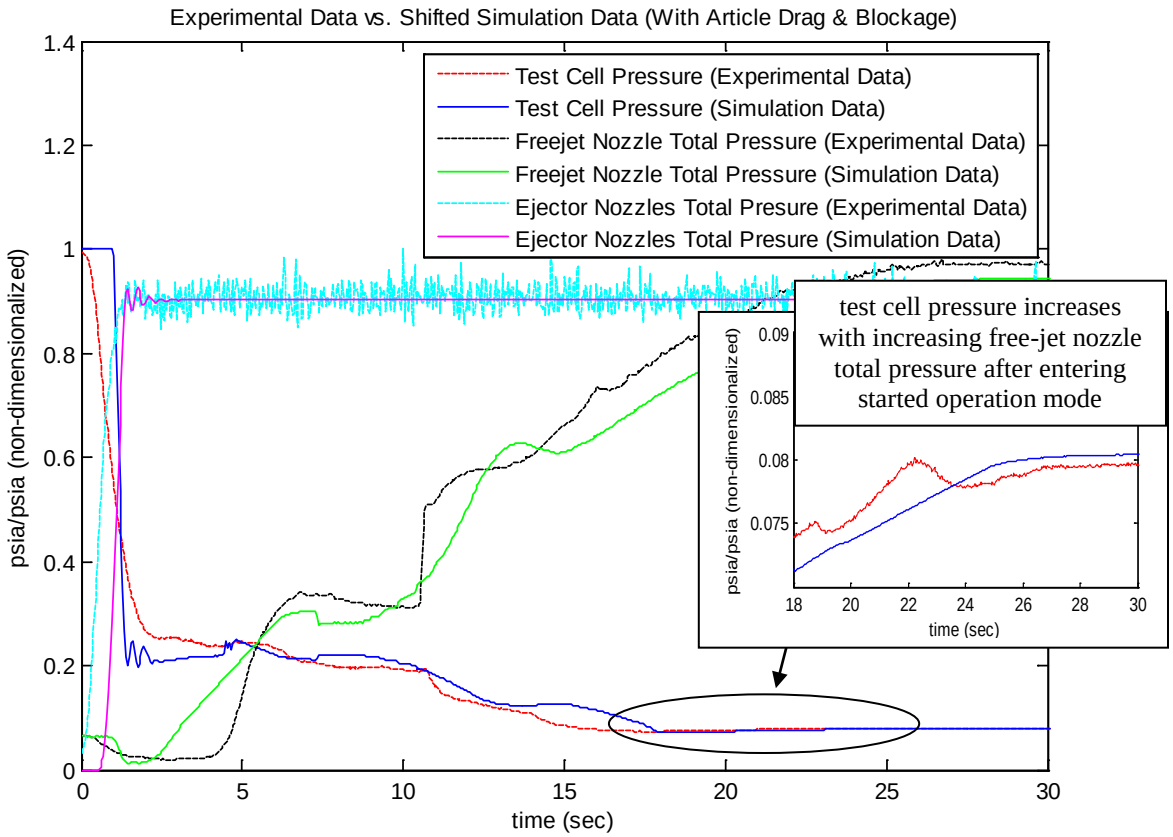

Figure 26: Experimental vs. Shifted Simulation Data (with Test Article Drag & Blockage

7. SUMMARY & CONCLUSIONS

A new computer model of the ejector diffuser system for a blow-down free-jet hypersonic propulsion facility was created that improved upon an existing ejector diffuser system model. The new model uses a 1-D mass and momentum balance method to calculate the airflow from the test cell which is modeled as a control volume with an assumed leakage area term. The previous model did not include effects of the test article, nor did it model the constriction of the secondary airflows by the free-jet and ejector nozzle plumes. It also did not include a normal shock pressure recovery factor for the ejector diffuser system. This resulted in an inaccurate simulation of the test cell pressure that would immediately drop down to a constant value upon the start of the ejector system flow. Then it would remain at this pressure and not respond to changes in either the ejector system or the free-jet nozzle total pressure.

A method for calculating the drag on the thrust stand and test article was implemented in the new model by deriving a (drag coefficient * Area) term from dynamic pressure and thrust stand scale force experimental data for a given test article. The (drag coefficient* Area) term can now be entered as a constant and multiplied by the dynamic pressure calculated in the simulation to get the drag force of the test article and the thrust stand at any point in time. A simplified ideal ramjet model was also implemented to calculate an estimate for gross thrust produced by the test article. This gross thrust is added to the drag calculated to get the net thrust from the test article/thrust stand. This contribution of force is added to the net force of all the flows in the ejector

diffuser system in order to calculate the flow needed from the test cell and thus the test cell static pressure.

In order to simulate the started mode of operation in which the test cell pressure actually increases as a function of a constant pressure ratio (test cell pressure / nozzle total pressure ratio), the nozzle flows and secondary flows past the nozzle were treated as two separate streams undergoing an isentropic expansion/contraction to attain the same pressure at the boundary of each flow. This was used to calculate an area of the secondary flow and thus a choked flow through this area. If the secondary flow from the test cell must be increased to this choked flow value in order to maintain a set pressure at the diffuser exit through a momentum and mass balance, then it has entered into a started mode of operation. Therefore, further increases in the driving ejector pressure (either the free-jet nozzle acting as an ejector or the ejector system nozzles) will result in the nozzle plume expanding out thus further constricting the area of the choked mass flow from the test cell. This results in the increase in test cell pressure due to the free-jet nozzle total pressure increasing after entering a started mode.

Finally, the new model incorporates a normal shock recovery correction of ~0.8 with ejector system and free-jet nozzle flowing; ~0.9 with ejector system only. This term accounts for the fact that in a supersonic diffuser, pressure recovery occurs through a system of oblique shocks which provide less pressure recovery than a normal shock. In addition to this, it was found that the extreme high pressures and low temperatures of the ejector system flows had real gas effects that weren't negligible. So a method was implemented for calculating the real gas mass flow and force of the ejector nozzles.

Incorporating the new ejector diffuser model into the facility model improved the fidelity and accuracy of the model as compared with experimental test data while negligibly affecting the speed of the facility model. Comparisons were made to some experimental test data that show a tight fit for both the final test cell pressure attained at operating conditions as well as the response of the test cell pressure to the ejector and free-jet nozzle total pressures. It accurately simulated both the unstarted and started modes of ejector flow, in which test cell pressure increases with nozzle total pressure once started.

8. RECOMMENDATIONS

The work completed for this thesis helped to further refine the accuracy of the facility model but further comparisons should be made with test data. When comparing experimental data with the computer facility simulation data, only one fixed ratio free-jet nozzle was modeled. Even though this computer model will work for any free-jet nozzle, further comparisons would help further validate the model.

Another recommendation is to better understand the mixed phase flow of the high pressure ejector flows. Although the model does not incorporate two phase flow effects while still comparing closely with experimental data, it would still be useful to understand the two-phase effects on the ejector diffuser system. Also, looking into the effects of the boundary layer on the ejector nozzle flows would be valuable since the effects could be larger than the real gas effects.

LIST OF REFERENCES

1. Nagaraja, K. S., and Hammond, David L., "One-Dimensional Compressible Ejector Flows", AIAA Paper 73-1184, Nov. 1973.

2. Bauer, R. C., Muse, W. W., and Tinsley, C. R., "Simulation of Flow Approaching the Chin Inlet of a Ramjet Missile", AEDC-TR-74-5, July 1974.

3. German, R. C., and Bauer, R. C., "Effects Of Diffuser Length On The Performance Of Ejectors Without Induced Flow", AEDC-TN-61-89, Aug. 1961.

4. Dutton, J. C., Mikkelsen, C. D., and Addy, A. L., "A Theoretical and Experimental Investigation of the Constant Area, Supersonic-Supersonic Ejector", AIAA Paper 81-0260R, Oct. 1982.

5. Luce, Richard W. and Jarvinen, Philip O., "An Approximate Method for Predicting Plume Sizes for Nozzle Flow into Still Air", AIAA Journal, Vol. 6, No. 1, pg. 182-183, 1968.

6. German, R. C., Bauer, R. C., and Panesci, J. H., "Methods for Determining the Performance of Ejector-Diffuser Systems", Journal of Spacecraft and Rockets, vol. 3 no. 2, pg. 193-200, Nov. 1964.

7. Ferri, A., *Elements of Aerodynamics of Supersonic Flows*. New York: The Macmillan Company, 1949.

8. Bauer, R. C., Matkins, E. H., Barebo, R. L., and Armstrong, W. C., "A Theoretical and Experimental Study of a Jet Stretcher System", Journal of Spacecraft and Rockets vol. 10 no. 6, pg. 395-405, June 1973.

9. Matz, R. J., and Kraft, E. M., "Investigations of Free-Jet Test Requirements and Techniques with Emphasis on the Adaptable Jet Stretcher", AEDC-TR-80-35, April 1981.

10. Mattingly, J. D., *Elements of Propulsion: Gas Turbines and Rockets*. Reston, Va.: American Institute of Aeronautics and Astronautics, 2006.

11. Anderson, J. D., *Modern Compressible Flow: With Historical Perspective*. New York: McGraw-Hill, 1990.

12. Porter, J. L., Squyers, R. A., "An Overview of Ejector Theory", AIAA Paper 81-1678, Aug. 1981.

13. German, R. C., Bauer, R. C., and Panesci, J. H., "Methods For Determining the Performance of Ejector-Diffuser Systems Used In Rocket Altitude Simulation", AIAA-1964-1428, Nov. 1964.

14. Ortwerth, P. J., "On the Rational Design of Compressible Flow Ejectors", AIAA Paper 78-1217, July 1978.

15. Cross, M. A., "Application of Computational Fluid Dynamics to Analysis of Exhaust Gas/Diffuser Interactions in a Turbine Engine Altitude Test Cell", AIAA Paper 87-2014, June 1987.

16. Roan, V., "An Ejector Performance Correlation Factor", AIAA Paper 91-2545, June 1991.

17. Sawaguchi, S., Ando, Y., and Hagiwara, K., "Experimental and theoretical investigation of the pressure recovery performance for an ejector-diffuser (supersonic flow)", AIAA Paper 96-2190, June 1996.

18. Gregory, David C., and Han, Sam, "Effects Of Multiple Primary Flows On Ejector Performance In An Ejector-Ram Rocket Engine", AIAA 2003-373, Jan. 2003.

19. Doe, Joe, "Improved Methods of Characterizing Ejector Pumping Performance", AIAA Paper 89-0008, Jan. 1989.

20. *Handbook of Chemical Hazard Analysis Procedures*, Appendix B, Federal Emergency Management Agency, U.S. Dept. of Transportation, and U.S. Environmental Protection Agency, 1989. Handbook of Chemical Hazard Analysis, Appendix B

21. Galanga, Fred L., and Mueller, Thomas J., "Cylindrical Diffuser Performance Using a Truncated Plug Nozzle", Journal of Spacecraft and Rockets 0022-4650 vol. 13 no. 4, pg. 254-256, Dec. 1975.

APPENDIX

ADDITIONAL FIGURES

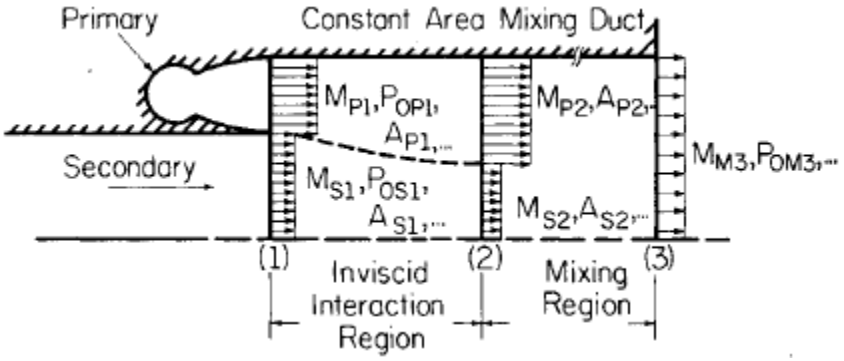

Figure 27: Ejector Flow Field Showing Compression of Secondary Flow (Internal Diffuser Choking) [4]

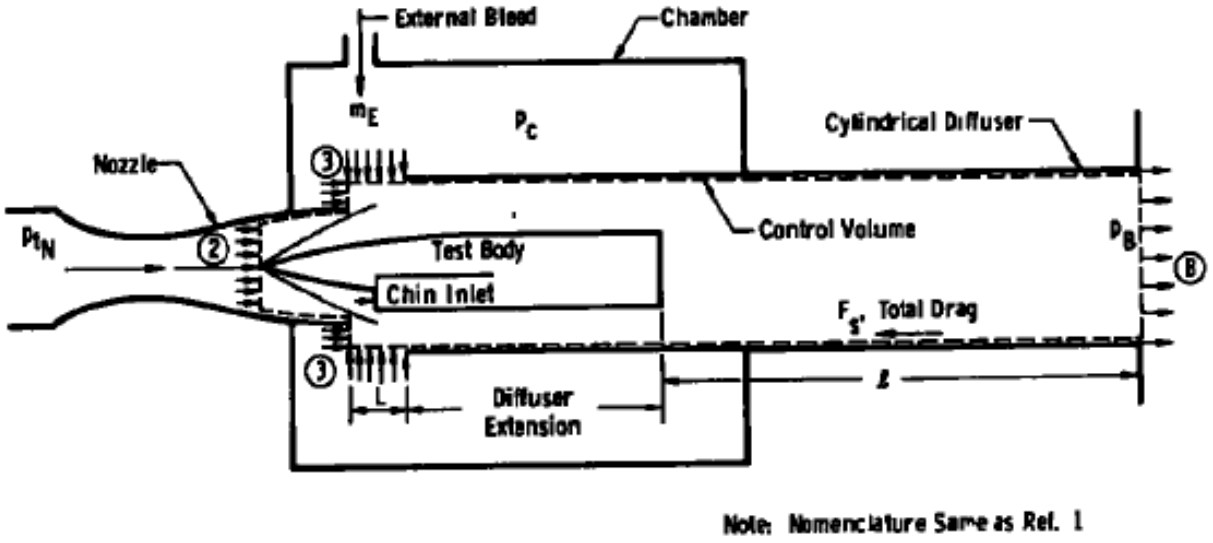

Figure 28: Sketch of Free-Jet Nozzle and Shroud [1]

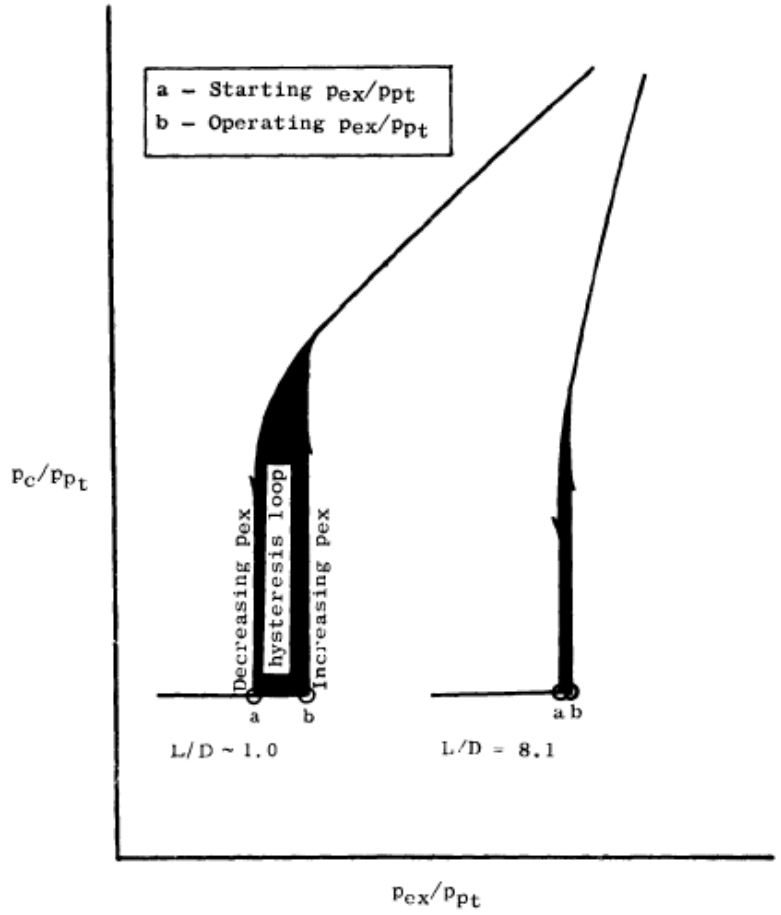

Figure 29: Effect of Diffuser Length-to-Diameter Ratio on Ejector Performance [3]

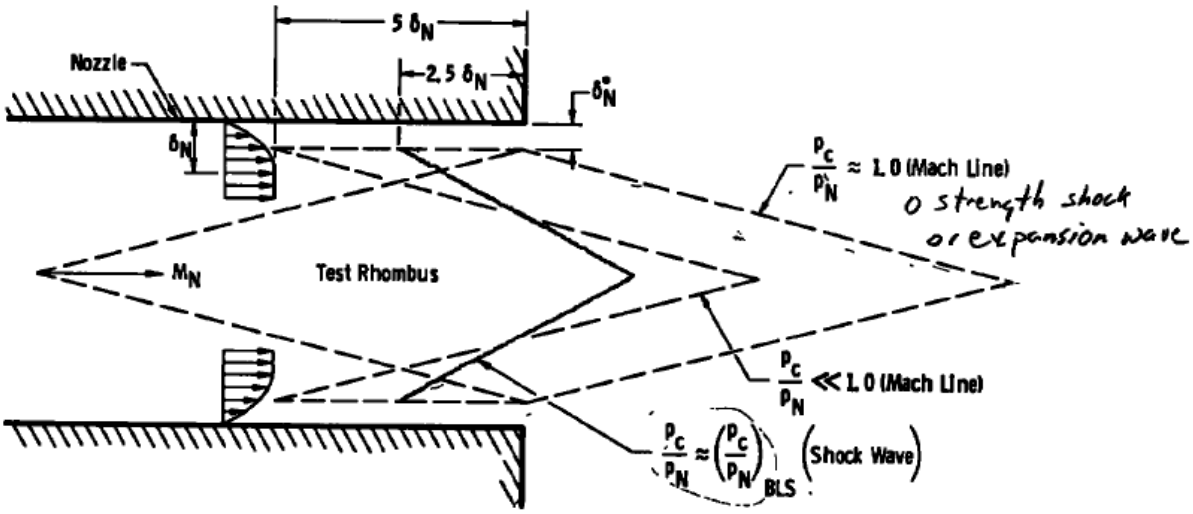

Figure 30: Variation of Test Rhombus with Chamber Pressure [1]

VITA

Derick Thomas Daniel was born in Lawrenceburg, Tennessee, in September 1983 to Mr. Mitchell Daniel and Mrs. Vickey Daniel. He attended Collinwood Elementary, Middle, and High School in his hometown of Collinwood, Tennessee. In 2001, he graduated High School and entered the University of North Alabama in Florence, AL. In Aug. 2003, he entered Tennessee Technological University in Cookeville, TN and received his Bachelors of Science degree in Mechanical Engineering in Aug. 2007 from this institution. During his time at Tennessee Technological University, he spent a year working as a co-op manufacturing engineer for Magotteaux Inc. in Pulaski, TN. After graduation, he started work for Aerospace Testing Alliance at Arnold AFB as a data analysis engineer in the Turbine Engine Testing department. He also enrolled in the graduate program at the University of Tennessee Space Institute that same semester.